LMSC-HREC TR D496846

Lockheed

Missiles & Space Company, Inc.

HUNTSVILLE RESEARCH & ENGINEERING CENTER

Cummings Research Park
4800 Bradford Drive,
Huntsville, Alabama

CONVECTION SENSITIVITY
AND THERMAL ANALYSES
FOR INDIUM AND INDIUM-
LEAD MIXING
EXPERIMENT (74-18)

May 1976

Contract NAS8-31671

by

S. V. Bourgeois
J. P. Doty

APPROVED: John W. Benefield, Supervisor
Advanced Technical Systems Section

FOREWORD

This report represents the results of work performed by the Lockheed-Huntsville Research & Engineering Center for the NASA-Marshall Space Flight Center under Contract NAS8-31671.

The NASA contract monitor for this investigation was Mr. Charles S. Schafer of the MSFC Space Sciences Laboratory.

ACKNOWLEDGMENT

The authors are grateful to Mr. Lawrence W. Spradley for helpful comments about the Thermal Analyzer Program and the Convection Computer Program and to Drs. J. H. McDermit[*] and P. G. Grodzka for their helpful comments, suggestions, and data interpretations. Mr. Charles S. Schafer contributed significantly with his helpful suggestions and ground based experimental data.

---

[*] Dr. McDermit now at McDonnell Douglas Company, Huntsville, Ala., and Dr. Doty at Eagle-Picher Company, Miami, Okla.

SUMMARY

Sounding rocket Experiment 74-18 was designed to demonstrate the effects of the Black Brandt rocket acceleration levels (during the low-g coast phase of its flight) on the motion of a liquid metal system. The experiment Principal Investigator was Mr. Charles S. Schafer of NASA-MSFC. This Lockheed-Huntsville study was performed primarily to assist the Principal Investigator in preflight design. Some post-flight analyses were also conducted.

Preflight studies consisted of heat transfer analysis and convection sensitivity and convection modeling analyses. These studies aided in the: (1) final selection of fluid materials (indium-lead melts rather than paraffins); (2) design and timing of heater and quench system; and (3) preflight predictions of the degree of lead penetration into the pure indium segment of the fluid. Postflight studies involved: (1) updating the convection sensitivity calculations by utilizing actual flight gravity levels; and (2) modeling the mixing in the flight samples.

Preflight convection sensitivity calculations were made for the cylinder perpendicular and parallel with the acceleration of gravity. The values for the Marangoni, Grashof, Prandtl, Rayleigh, Nusselt, solutal Rayleigh and Schmidt numbers, momentum diffusion time, and thermal conduction time are calculated for the melted indium. These sensitivity calculations indicate that:

- Expected convective heat losses, from the mixing cylinders to the ambient air, during rocket tests can be simulated by ground tests utilizing ambient air at 0.1 atm.

- Thermogravitational (including g-jitter) and thermocapillary convection will not induce mixing during the rocket tests.

- Solutogravitational and possibly solutocapillary convection will induce mixing during rocket tests.

In addition to sensitivity analyses, the heat transfer in the mixing experimental apparatus was mathematically modeled via a lumped parameter model (Lockheed-Huntsville Thermal Analyzer Computer Program). Graphs of the heat-up and quench were drawn which show the temperature history of the indium/indium-lead mixture. Based on these results, recommendations were made to move the quench time from 310 to 295 seconds (laboratory time point). The temperature gradients calculated were also used in the convection sensitivity studies.

The postflight sensitivity analyses confirmed rocket results because they indicated that Flight Sample No. 6 was most susceptible to convection; while the other two samples(Nos. 1 and 2) were subject to only marginal or no convective mixing. The analyses indicated that only solutal (concentration gradient) induced buoyancy and surface tension forces can induce stirring in the flight samples. The postflight modeling results, however, did not show significant mixing in any of the flight cases. These models only considered buoyancy forces. Thus, it is concluded that the large amount of mixing seen in Flight Sample No. 6 is the result of solutal surface tension forces or the result of unexpected solutal buoyancy forces. The latter is most probable and can be explained if the flight acceleration levels were higher than those used in this study and/or if a more rigorous (three-dimensional) computer model is utilized. It is recommended that further analysis of acceleration levels and that several additional cases of the present computer model be conducted to clarify the rocket flight results.

CONTENTS

Section 1

PREFLIGHT ANALYSES

This section presents the results of preflight thermal analysis and convection prediction portions of a theoretical investigation into the Indium and Indium-Lead Mixing Experiment for the Space Processing Rocket Program of NASA-MSFC (designated as Experiment 74-18). The phenomena being investigated are those which could induce flow by causes other than residual acceleration through the non-spin platform of the rocket system. In this first phase investigations were specifically directed to supporting the design, fabrication and flight sequence timing of the Mixing Experiment 74-18. Other theoretical phases of this program include convection calculations from various causes such as thermal gradients, surface tension, bubble convection, phase change and g-jitter. The results presented in this section include temperature histories of the metals during heat-up and quench and convection sensitivity calculations.

1.1 DESCRIPTION OF THE APPARATUS

The experimental system is a set of mutually perpendicular cylindrical samples which were melted, allowed to remain molten for about four minutes, then resolidified, all while in the low-g portion of the rocket flight. The samples were composed of two cylindrical sections joined together; one section was pure indium, the other was 80% indium and 20% lead (by weight). This gives a density difference of about 7% between the two liquids.

The mixing apparatus[*] is basically an aluminum cylinder 0.614 cm i.d. and 3.68 cm long which is closed and sealed at both ends by aluminum caps. One-half of the free length of 2.5 cm is filled with indium metal except for an

---

[*]Engineering drawings of the mixing apparatus are shown in Figs. A-1,-2 and -3.

air space at the end for expansion. The other half is filled with an alloy of indium 20% lead except for the expansion air space. The inner end surfaces of the metal and the alloy touch at the midpoint along the length of the cylinder and are held in position by "smoked" aluminum rings at each end of the cylinder.

The indium and indium-lead are heated past the melting point by a nichrome heater wire wound around the cylinder. This heater wire has a stainless steel sheath and is electrically insulated from the sheath by magnesium oxide powder. There are $29\frac{1}{2}$ turns wound around the cylinder and the heater wire then goes directly to a terminal on the mounting bulkhead.

The cylinder is held in position and supported by a thin stainless steel bracket which is welded to the heater wire sheath and attached to the mounting bulkhead. Also mounted to this bulkhead are two other (identical) cylinders whose axes are perpendicular and are also mutually perpendicular to the first cylinder's axis. These two cylinders are supported by a single mounting bracket, while the other cylinder is mounted by a single bracket. These three cylinders, heaters, mounting brackets and bulkhead are contained inside a cylindrical chamber with a void volume of approximately 571.8 cc.

In order to resolidify the metal and alloy very quickly a supply of water is carried in an elastic bladder attached at one end of the cylindrical chamber. The contained water is released at 295 sec (laboratory time) after the heater is turned on, and is rapidly expelled into the chamber by water pressure which is created by the elasticity of the bladder. There is an excess of water in the bladder which ensures that a large percentage of the chamber will be filled. An air relief tube vents the air behind the bladder as the chamber is being filled. The water which is filling the chamber, is in motion and exposes the heaters to fresh cold water almost continuously. This will quench the molten metal and alloy before the rocket payload experience high-g forces upon reentry.

There are two time frames in which this experiment can be investigated; one is the rocket time frame; the other is the laboratory time frame. These are compared in the following table.

2

Event After Rocket Firing	Rocket Time Frame (sec)	Laboratory Time Frame (sec)
Heat Turned On	45	0
Heater Turned Off	225	180
Water Quench Initiated	340	295
High-g Experienced	405	360

All times given in this report will be in the laboratory time frame unless otherwise specified.

1.2 THEORETICAL THERMAL ANALYSIS

In order to investigate the heat transmission from the heater to the indium metal and the indium-lead alloy a mathematical model of the mixing apparatus had to be made. The partial differential equations to be solved which would describe the transmission of heat by conduction through the apparatus, are sufficiently complicated that a discrete model and computer solution is needed. The best type of discrete model is the lumped parameter model. From the engineering drawings a lumped parameter model was developed which considered the geometry, materials and heater of the mixing apparatus. The math model was made with the least amount of deviation from the actual apparatus. The correct dimensions, density, thermal conductivity, and specific heat for each material were used. In the case of the indium and indium-lead and the surrounding air, each were dimensionally subdivided in order to obtain better thermal gradients and conduction patterns. The lumped parameter modeling method assumes that the model is divided into cells so that the properties of a particular cell may be stated as existing at the center of the cell or at its surfaces. This method leads itself to the solution of complicated problems that involve partial differential equations which describe the behavior of physical parameters. Thermal conduction is one such problem and the temperature is a parameter of interest.

The model has the indium solid cylinder divided into six pieces; two radial sections by three longitudinal sections. The indium-lead alloy is also subdivided in a like manner. An air space has been left at the outer ends of the solid cylinders for expansion. The aluminum end caps have each been

3

subdivided into two longitudinal pieces. The aluminum cylinder was not subdivided and is considered to have exactly the same dimensions as shown in the engineering drawings.

The heater wire which is wound around the cylinder $29\frac{1}{2}$ turns has been modeled as a set of concentric thin cylinders. The heater wire is nichrome with a stainless steel sheath and a magnesium oxide electrical insulation powder packed in between the nichrome wire and the sheath. Since the stainless steel sheath is very thin, the heat is conducted through it fast, so it can be represented as a cell of zero thickness. In order to account for the distance the thickness of the sheath is added to the thickness of the magnesium oxide. This simplification of the heater model was checked by leaving the sheath in the calculations and comparing the resulting temperatures, which were almost the same in both cases. So, the heater was modeled as three concentric cylinders; the inner one of MgO; the center one of nichrome; the outer one of MgO.

The air was subdivided into a number of concentric cylindrical rings around the heater and at the ends of the cylinder and heater. The air extended 2.5 cm in an axial direction from the end of the cylinder and heater, and it extends a total of 3 cm radially from the centerline of the cylinders. A "cold wall" ($22^{\circ}C$) heat sink was placed at the outer edge of the air and completely surrounding all the air.

During the testing portion of the lumped parameter model, a number of different computer trials were made using various model configurations. In one such trial the holding bracket was included; in another the radiation was considered. In still a different trial an effective thermal conductivity for air was used to consider convection at 1g. Since one of the ground tests was run in a vacuum chamber at 0.10 atmosphere of pressure, a computer trial was used to approximate the convective-conductive air at this pressure. In this case an effective thermal conductivity was calculated and used which considered convection at 0.10 atmosphere and the thermal conduction in air.

To effect the water quench the computer program was stopped at the 295 second step, and values for water were substituted for the air. With the

4

air replaced by water which was a heat sink (because the temperature would only rise 3.8°C) the model was run on the computer until the 360 second step.

In the lumped parameter model the temperature of a particular cell is taken at the center of that cell. Also considered at the center of the cell is the thermal capacity of the cell's volume. To propagate the heat by conduction each cell is connected by a heat flow resistance. This resistance is inversely proportional to the thermal conductivity of the cell and inversely proportional to the bounding area of the cell through which the heat must be conducted. This resistance is directly proportional to the path length which is the distance between centers of the two connecting cells. Radiation is directly proportional to the fourth power of the temperature differences. Thus, the parameters of the lumped model are defined at the center of the cell, at the surface of the cell, and by cell interconnecting parameters.

Physical problems solved through a lumped parameter model yield realistic solutions that match closely to experimental results. The lumped parameter model is illustrated as Fig. 1. The thermal properties of the materials in the mixing apparatus are given in Tables 1 and 2 (utilizing Refs. 2, 3, 4, 5).

1.3 THERMAL ANALYZER COMPUTER PROGRAM

Prior to this project Lockheed-Huntsville developed a computer program which was used to solve heat transfer systems. The Thermal Analyzer computer program utilizes a finite difference technique to solve the general heat balance equation for systems in zero or low gravity. The lumped parameter model thereby lends itself to easy solution by the Thermal Analyzer program.

The general heat balance equation that this computer program solves for special cases is (Ref. 1):

$$T_{i,\theta+\Delta\theta} = T_{i,\theta} + \left[\sum \frac{T_{j,\theta}}{R_{ij}} - T_{i,\theta} \sum \frac{1}{R_{ij}} + \bar{Q}_{i,\theta+\Delta\theta} \right] \frac{\Delta\theta}{C_i}$$
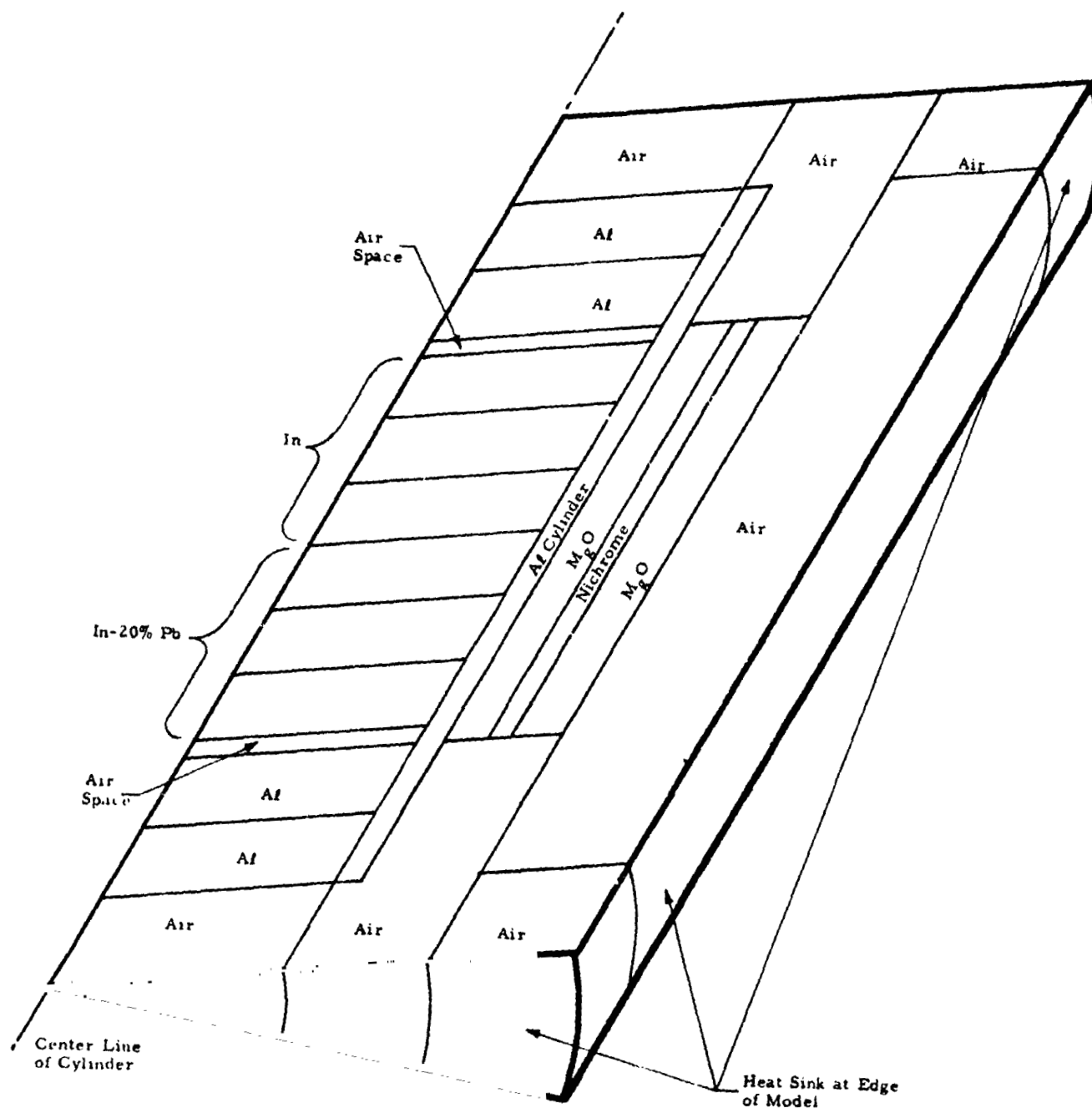
5

Fig. 1 - Illustration of the Lumped Parameter Model

Table 1

THERMODYNAMIC PROPERTIES[*] OF THE MATERIALS
IN THE MIXING APPARATUS

Material	ρ	k	C_p
In (156.4°C M.P.)	7.25	0.06	0.058
In-Pb (20%) (160°C M.P.)	8.07	0.064	0.053
In (liquid)	7.02	0.10	0.0654
In-Pb (20%) (liquid)	7.82	0.088	0.0596
Al 6061-T6	2.80	0.35	0.211
Quartz	2.65	0.023	0.0165
Cu	8.94	0.948	0.0922
Nichrome	8.247	0.032	0.107
MgO	3.58	0.0002	0.24
Stainless Steel 347	7.85	0.088	0.125
Stainless Steel 304	7.85	0.088	0.125
Air	0.0012	62.2×10^{-6}	0.238
Water	1.0	0.0015	0.998
Eicosane (36.8°C)	0.841	35.6×10^{-5}	0.530
Octacosane (61.4°C)	0.912	35.6×10^{-5}	0.511
Eicosane (liquid)	0.744		
Octacosane (liquid)	0.756		

[*]CGS units; ρ = density; k = thermal conductivity; C_p = heat capacity.

Table 2

PHYSICAL PROPERTIES OF LIQUID INDIUM
AND INDIUM-LEAD

Property (units)	Symbol	Value* for In	Value* for In-Pb
Dynamic Viscosity (poise) (gm/cm/sec)	μ	0.012	
Kinematic Viscosity (stokes) (cm^2/sec)	ν	1.7×10^{-3}	
Surface Tension (dyne/cm)	σ	340.0	
Change of σ with Temperature (dyne/cm/^{o}C)	$\frac{d\sigma}{dT}$	-0.08	
Volumetric Expansion Coefficient (cm^3/cm^3/^{o}C)	β	1.15×10^{-4}	
Thermal Diffusivity (cm^2/sec)	α	0.218	
Impurity Concentration (mole/mole)	C		$0.20 - 0.23$
Change of Density with Concentration	$\beta_c = \frac{1}{\rho}\left(\frac{\partial \rho}{\partial C}\right)_T$	0.497	
Mass Diffusivity (cm^2/sec)		$1\text{-}3 \times 10^{-5}$	
Heat of Fusion (cal/gm)		6.8	6.6
Radius of In (or In-Pb) (cm)	r(H)	0.307	0.307
Length of In and In-Pb (cm)	L(H)	2.35	
Mass (gm)	ρV	2.52	2.80
Gravity at 10^{-4}g (cm/sec^2)	g		9.8×10^{-2}

*All values are given in CGS units.

8

where

T_i = the temperature for the ith cell

θ = the time variable

$\Delta\theta$ = time increment

R_{ij} = resistance to thermal conduction between the ith cell and the jth cell.

$\overline{Q}_i$ = average heat rate over the time increment $\Delta\theta$ (cal/sec) (heat added from the heater or taken up by a heat sink)

C_i = heat capacitance of the ith cell

where

$$R_{ij} = \frac{L}{kA}$$
$$C_i = \rho V C_p$$

and

L = effective conduction path length between cells (cm)

k = thermal conductivity of the cell's material

A = effective cross-sectional area for heat transfer between two cells

ρ = density of the cell's material

C_p = specific heat of the cell's material

V = volume of the cell (cm^3)

Radiative heat transfer computed from equation:

$$Q_{rad} = \sigma A_r \mathscr{F}_{ij} [T_i^4 - T_j^4] \left(\frac{cal}{sec}\right)$$

where

σ = Stefan-Boltzmann constant (cal/sec-cm^2-($^\circ$K)^4)

A_r = effective radiating area (cm^2)

$\mathscr{F}$ = effective view and emissivity factors

T_i = absolute temperature of the ith cell ($^\circ$K)

9

The radiative resistance is calculated by

$$R_r = \frac{1}{A_r \, \mathscr{F}_{ij}(T_i^2 + T_j^2)(T_i + T_j)}$$

which is used in the resistive parts of the general heat transfer equation.

The Thermal Analyzer program computes new temperatures for each cell in time step increments. An iterative method is used to achieve accurate results in solving the heat transfer equation for each cell. Thus, very accurate temperatures can be calculated for each cell of the lumped parameter model at certain time increments. The time increments are computed by the program and are determined by the stability of the solution. In this particular case of the mixing apparatus, the time step was 0.0015 sec, or 667 steps to equal 1 second of the laboratory time.

1.4 THERMAL RESULTS

Entering the lumped parameter model into the Thermal Analyzer program yields a time-temperature trace of the mixing apparatus. The program calculates and prints out the temperature of each and every cell, from 0 sec to 360 sec in increments of 5 sec.

The heat rate put out by the heater was hand-calculated by the equation

$$Q = \frac{E^2}{4.18\,R} \quad cal/sec$$

where the applied voltage on the heater was 28 volts and the heater resistance for one heater is 46.5 ohms. This yields 4.03 calories per second heat input from the heater wire. This quantity of heat was input in the nichrome wire of the lumped parameter model.

10

The phase change at the melt time was hand calculated so that fewer computer runs could be made. The calories required to melt the indium metal and the indium-lead alloy is:

$$q_{In} = (\rho V H_f)_{In}, \qquad q_{In-Pb} = (\rho V H_f)_{In-Pb} \quad (cal)$$

where

ρ = density

V = volume

H_f = latent heat of fusion

The subscript In and In-Pb designate quantities used in the paranthesis are for indium and indium-lead respectively. Assume that one-half of the heat input goes to the air and heat sink (which is close to that value computed by the computer program), and that all influx of heat at the time of melt goes to melting the metal. The time for melting is calculated from

$$t_m = \frac{q}{\frac{1}{2} Q} \quad (sec)$$

where

Q = heat rate input from the heater wire.

These calculations yield a melt time for the indium of 8.49 sec and a melt time for the indium-lead of 9.17 seconds. Since there is approximately $3.6^\circ C$ between the melt points and thus only 2 seconds of duration occur after the indium melts, the two melt times can be additive. The time element between melts is also shortened by heat input to both so that the indium-lead alloy will probably begin melting before the pure indium has completely melted. These effects would tend to cancel thus yielding a total melt time of approximately 17 seconds. Only the melt time for the indium is plotted in the following graphs.

11

These graphs, shown in Fig. 2, are the temperature versus time plots for indium only. The graphs are for the cell which is located at the outer edge near the air gap and at the center of the cylindrical cell. The hand calculated melt time for indium is added to the computer calculated temperature history to yield a complete curve. The curve for the indium lead is almost identical except for the melt temperature.

1.5 TEMPERATURE VS TIME GRAPHS

Three different cases were investigated: (1) low loss case; (2) typical case; and (3) highest heat leak possible case. These different cases were considered because cases (1) and (3) should bracket the actual flight experiment, and the typical case lies between them. The low loss case considers the smallest heat leak that the experiment will probably have. For this minimal heat loss case only the bulkhead and the container are considered but they are considered not to gain heat. Thus, a "cold wall" heat sink at 22°C is considered to surround the heater and cylinder at the outer edge of the air. In this case the only heat lost is that which is conducted through the non-convective air to the wall.

The typical case considers the "cold wall" along with a holding bracket and radiation to the wall of the container. The bracket in the typical case was modeled as a combination of the two brackets used to hold the three different mixing cylinders and heaters. One of the actual brackets is longer than the other and it holds two of the cylinders while the shorter one holds only one cylinder. Radiation losses are also considered from the exterior of the heater and cylinder to the bulkhead and the container walls which are 22°C. The heat loss values[*] are:

- "Cold Wall" ~ 2%
- Through the Bracket ~ 3%
- By Radiation to the "Cold Wall" ~ 4%.

The highest heat leak case considered the "cold wall," bracket and radiation again, but the bracket in this case was shortened and mounted on a heat

---

[*] Fraction of convective heat loss to surrounding air.

A = Time the heater is turned "on"   D = Time that high-
B = Time the heater is turned "off"   E = Temperature of
C = Time the quench is started   F = Temperature of
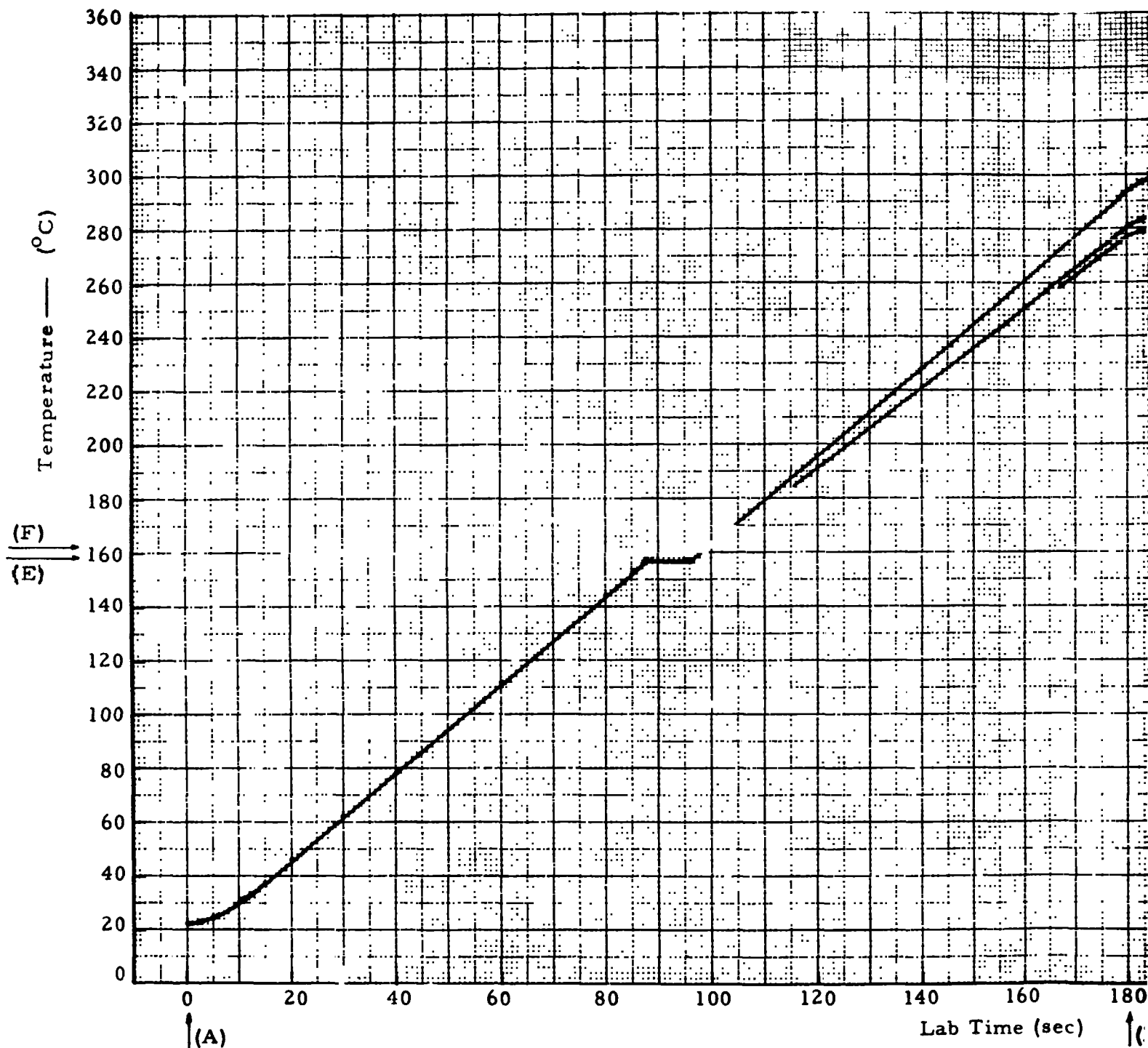
FOLDOUT FRAME /

Time that high-g levels are experienced
Temperature of Indium melt point
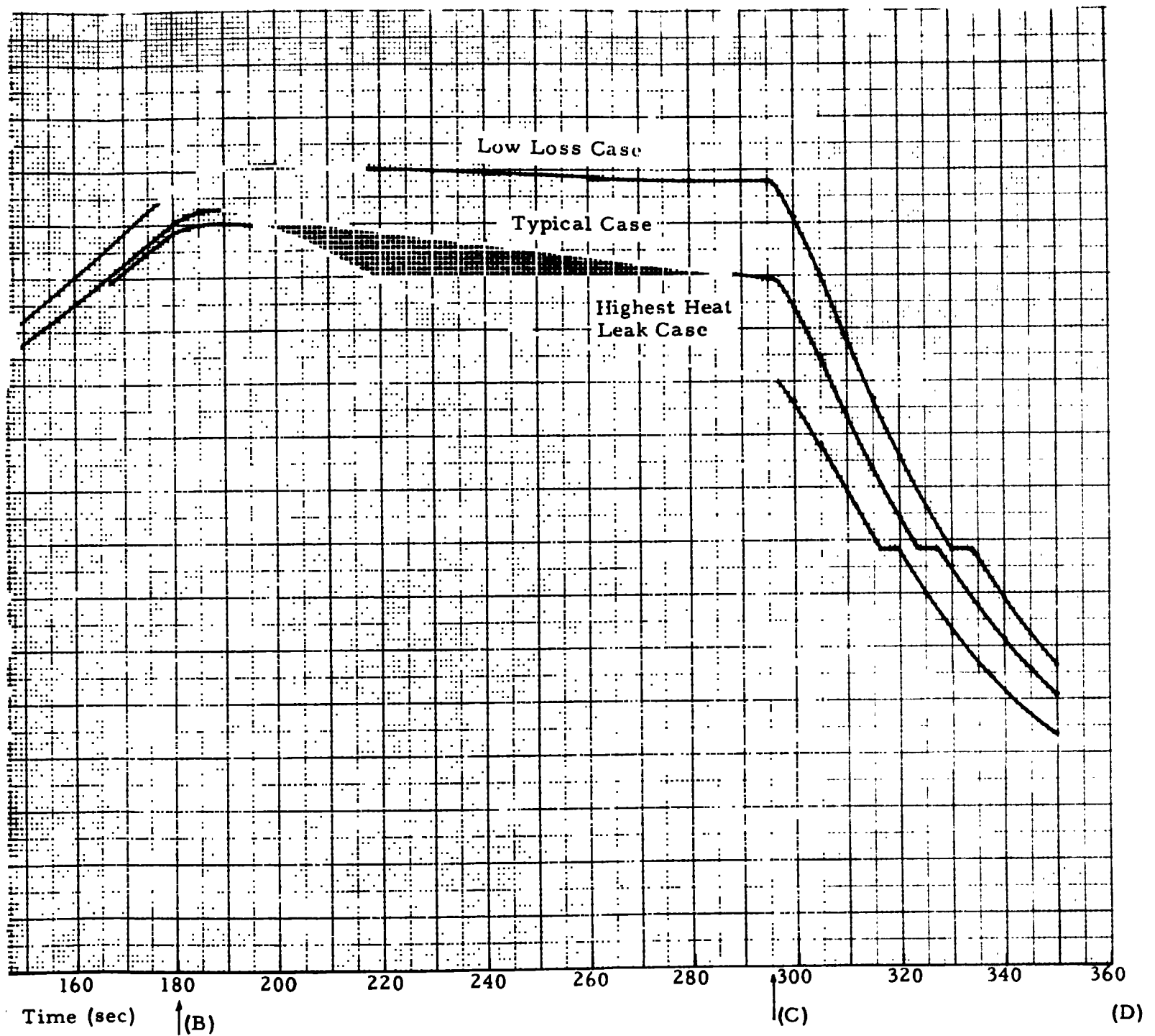Temperature of Indium-20% Lead melt point

Fig. 2 - Time-Temperature Curve for
Indium at Low/Zero-g

sink bulkhead. This bracket was modeled after the shortest of the two brackets which only holds one heater and cylinder. The bulkhead to which it is attached, was considered as a heat sink at 22°C. The heat loss rate through this bracket was approximately at a 10% rate, which is 2.5 times more than that lost from the typical case bracket. Again radiation and the "cold wall" contributed 4 and 2%, respectively, to the heat loss rate.

The water quench was modeled by substituting water for the air. This was accomplished by substituting water specific heat, conductivity and density for those same properties for air. The temperature of the water was set and held at 22°C which made the water a heat sink. The initial temperature of each cell, except the cells occupied by water, was taken from the heat-up, computer run at 295 sec of lab time. There was a quench computation made for each of the three cases. The duration of the phase change during the quench was calculated from the slope, which yielded 3.8 sec.

One further case that was computed was that of convective air at 0.10 atmospheres of pressure. This case was computed in order to match the conditions of a ground test which was made in a vacuum of 0.10 atmospher.s. The Nusselt number for 1 g and air density of 0.1ρ was calculated and yielded 3.88 which is 31.6% of that of air at one atmosphere and 1 g. Since the Nusselt number is the ratio of the convective heat transfer to the conductive heat transfer, the thermal conductivity of the air was modified by a multiplicative factor of (1 + 3.88). The air then has it's usual thermal conductivity plus the convection due to 1 g and a pressure 0.10 atmosphere. The temperature-time graph (Fig. 3) of this case matched very well the data obtained in the vacuum ground test. The test data are not yet available in graph form, thus the data are not shown in Fig. 3. This vacuum ground test was conducted to simulate convective heat losses (from the cylinders to the ambient air) during rocket testing.

1.6 THERMAL GRADIENTS

The graphs shown in Figs. 2 and 3 are for one typical cell of indium; however, each cell of the indium and the indium-lead is very near this temperature
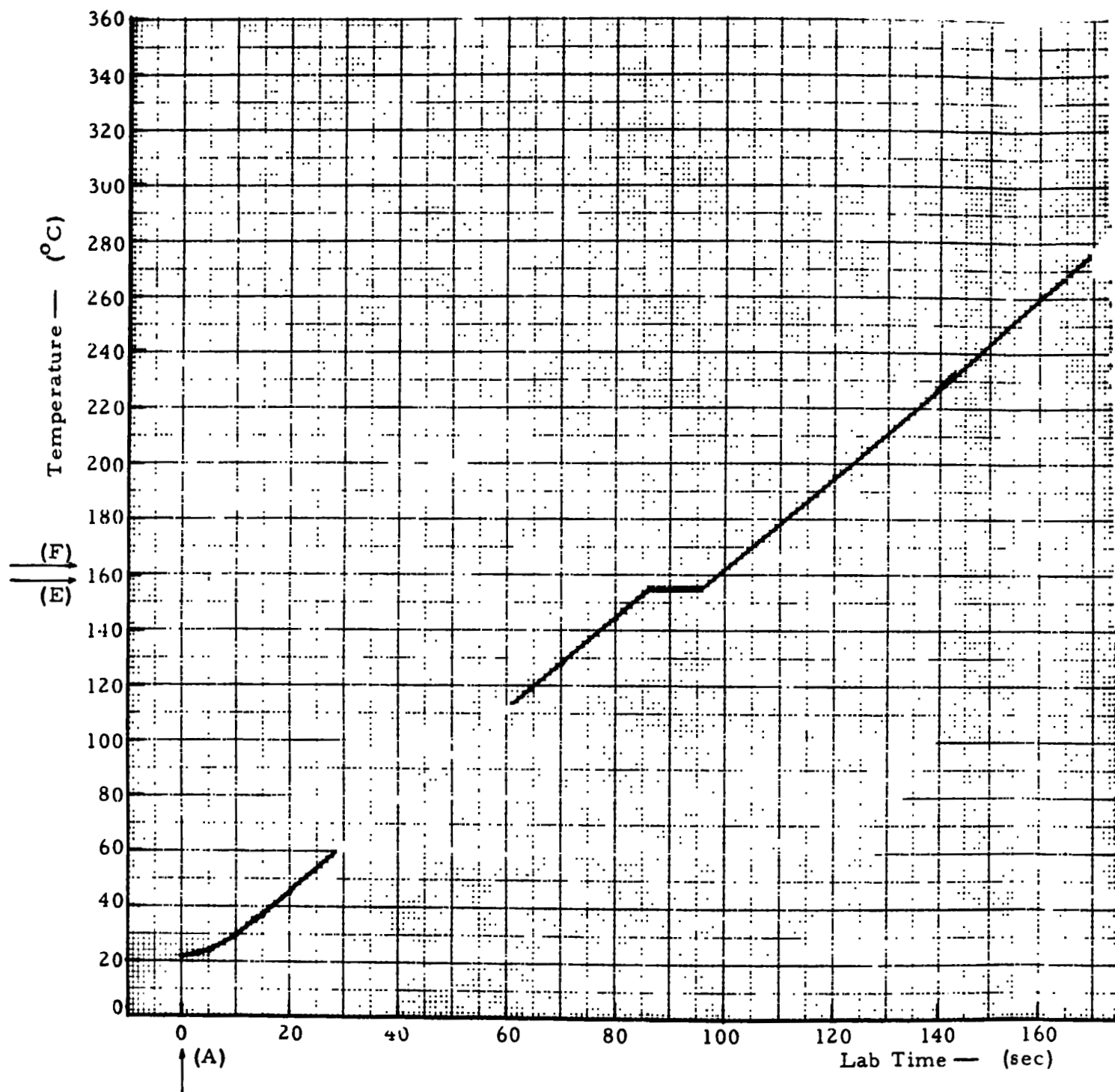
A = Time the heat is turned "on"   E = Temp

B = Time the heater is turned "off"   F = Tempe

C = Time the quench is started

E = Temperature of Indium melt point

F = Temperature of Indium-20% Lead melt point

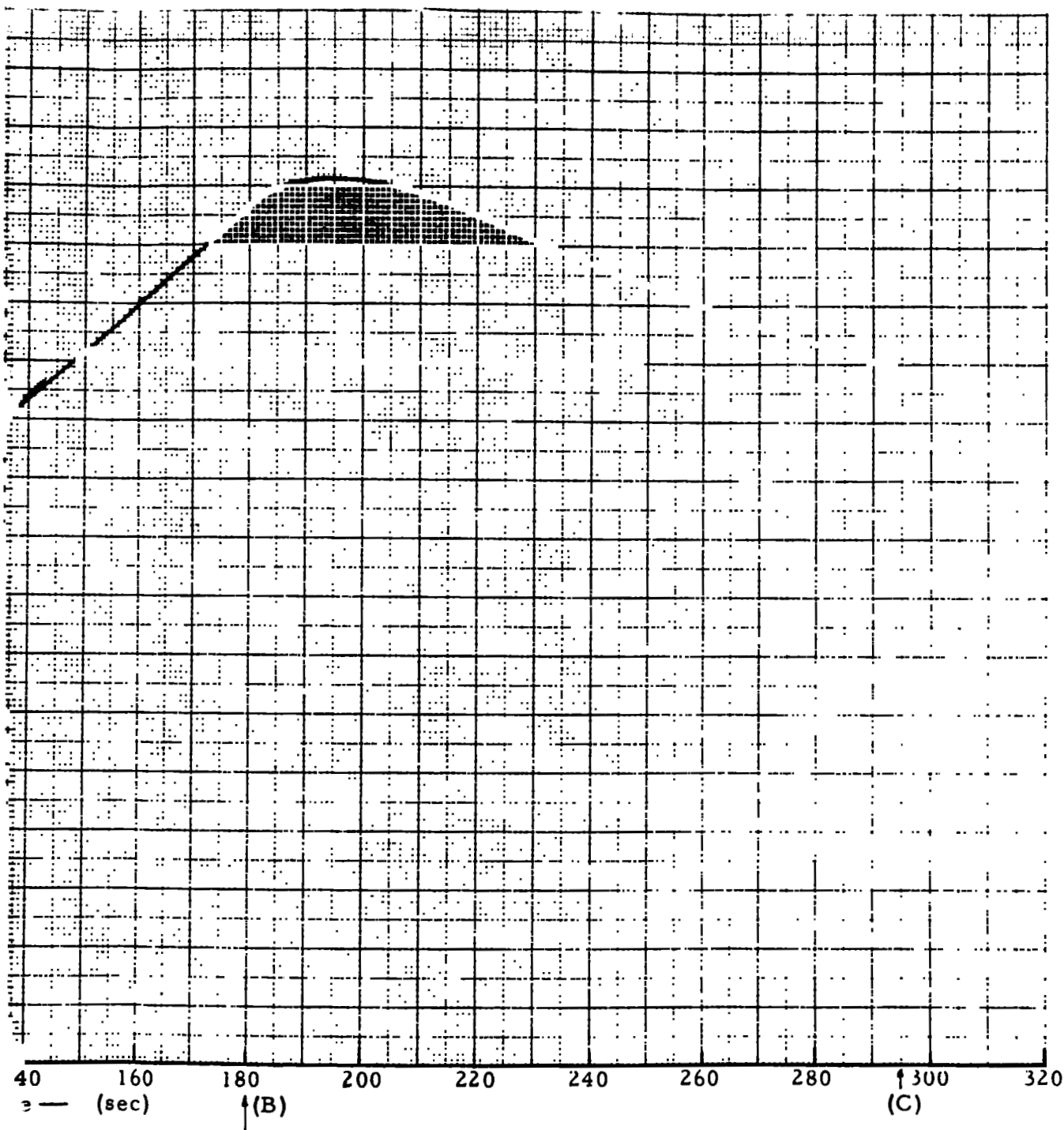40   160   180   200   220   240   260   280   ↑300   320

ᵧ— (sec)   ↑(B)   (C)

Fig. 3 - Time-Dependent Curve for
Indium at 1 g and Surrounding
Air Pressure of 0.10 atm

15

FOLDOUT FRAME

curve. The temperature gradients are small even over the total length of the cylinder. Since the heater is wound around the cylinder, the temperatures are assumed to be symmetric about the cylindrical axis. For this reason the maximum thermal gradient would be from the outside to the cylindrical axis, so that the radius is the characteristic length. The maximum thermal gradient along the cylindrical axis is from one end to the other end. The following tables gives the temperature gradients.

Max. Thermal Gradient for:	Temperature (^{o}C)	Temperature (^{o}C)	ΔT (^{o}C)	Distance (cm)	$\frac{\Delta T}{\Delta X}$
Radial	308.353	308.655	0.302	0.307	0.98
Longitudinal	308.262 (In)	308.289 (In-Pb)	0.027	2.35	0.011
Across In--In-Pb (ave) Interface	308.506 (In)	308.530 (In-Pb)	0.024	0.782	0.031
Across In--In-Pb (max) (next to axis)	308.440 (In)	308.475 (In-Pb)	0.035	0.782	0.045

1.7 CONVECTION SENSITIVITY CALCULATIONS

This section is subdivided into three parts: (1) equations for the various dimensionless numbers; (2) air convection on the outside of the apparatus; and (3) indium and indium-lead convection inside the cylinder.

1.7.1 Dimensionless Numbers

The following dimensionless numbers are calculated throughout this section:

$$\text{Grashof number, Gr} = \frac{(\text{Bouyancy Forces})}{(\text{Viscous Forces})}$$

$$\text{Prandtl number, Pr} = \frac{\text{Momentum Transport}}{\text{Heat Transport}}$$

Rayleigh number, Ra $= \dfrac{(\text{Buoyancy}^* \text{ Forces}) \times (\text{Moment Transport})}{(\text{Viscous Forces}) \times (\text{Heat Conduction})}$

Nusselt number, Nu $= \dfrac{\text{Convective Heat Transfer}}{\text{Conductive Heat Transfer}}$

Marangoni number, Ma $= \dfrac{\text{Surface Tension Driving Forces}}{\text{Viscous Forces}}$

Solutal Rayleigh number, Ra' $= \dfrac{(\text{Buoyancy}^{**} \text{ Forces}) \times (\text{Momentum Transport})}{(\text{Viscous Forces}) \times (\text{Mass Diffusion})}$

Schmidt number, Sc $= \dfrac{\text{Kinematic Viscosity}}{\text{Mass Diffusivity}}$

Critical Rayleigh number, Ra_c $=$ Point at which convection begins to augment mass diffusion or thermal conduction; i.e., mixing begins

The equations for each of these dimensionless numbers are:

$$Gr = \frac{g \Delta T \, H^3 \beta}{\nu^2}$$

$$Pr = \frac{\mu C_p}{k}$$

$$Ra = Gr \; Pr$$

$$Nu = \frac{h H}{k}$$

$$Nu = 0.525 \, (Ra)^{1/4} \quad \begin{array}{l}\text{for convection external to a}\\ \text{horizontal cylinder (Refs. 5,6 and 7)}\end{array}$$

$$Ma = \frac{\frac{\partial \sigma}{\partial T} \Delta T \, H}{\rho \nu \alpha}$$

---

*Temperature gradient induced (thermal or thermogravitational)

**Concentration gradient induced (solutal or solutogravitational)

$$Ra' = \frac{\beta_c \, g \, \Delta C \, H^3}{D\nu}$$

$$Sc = \frac{\nu}{D}$$

where

H = characteristic length*

T = temperature

ΔT = incremental change of temperature

g = gravitational acceleration

ρ = density

μ = dynamic viscosity

ν = kinematic viscosity

σ = surface tension

α = thermal diffusivity

D = mass diffusivity

C = concentration of solute

ΔC = incremental change of solute concentration

k = thermal conductivity

C_p = specific heat

β = volumetric thermal expansion

h = heat transfer coefficient

The following two-time constants are calculated for indium and indium-lead.

$$t_{md} = \frac{H^2}{\nu} \text{ , momentum diffusion time (3250 sec of In Pb)*}$$

$$t_{td} = \frac{H^2}{\alpha} \text{ , thermal conduction time (25.3 sec for In Pb)*}$$

1.7.2 Air Convection

In order to compare the heat transfer and the convection of the air at various levels of gravitational acceleration, the Grashof, Rayleigh and Nusselt

---

*H = 2.54 cm.

18

numbers are calculated for various g levels. The following table (from Refs.6 and 7) shows the dimensionless numbers for the air surrounding the cylinder under various gravity conditions.

Acceleration	Grashof Number	Rayleigh Number	Nusselt Number
1g	4.37×10^5	2.98×10^5	12.26
0.1g	4.37×10^4	2.98×10^4	6.90
$10^{-3}g$	4.37×10^2	2.98×10^2	2.18
$10^{-4}g$	4.37×10^1	2.98×10^1	1.23

A ground test was made with 0.10 atmospheres of pressure surrounding the mixing cylinders and inside the container. In order to make a comparison between the actual ground experiment and the computer model, a Nusselt number was calculated for 0.10 atmospheres. These calculations resulted in:

1 g and air at 0.10 atmosphere of pressure

$$Gr = 4.36 \times 10^3$$
$$Pr = 0.682$$
$$Ra = 2.98 \times 10^3$$
$$Nu = 3.88$$

$$\frac{Nu\,(0.1\ atm)}{Nu\,(1.0\ atm)} = 0.316$$

$$\frac{Nu\,(0.01\ atm)}{Nu\,(1.0\ atm)} = 0.1$$

The Nusselt number was used to modify the air parameters for conductive and convective air under these conditions. This was done by multiplying the thermal conductivity by $(1 + 3.88)$ or $k' = k\,(1 + 3.88)$.

19

1.7.3   In-Pb Convection Sensitivity

A simple, reliable estimate of whether convection exists, and its strength, can be obtained from dimensional analysis. This is especially true for thermogravitational flows which have been studied extensively (both theoretically and experimentally) for the past 30 years (Ref. 8). The analysis of thermocapillary flows, however, is not as extensive due to the difficulty of suppressing the usually dominant buoyancy forces during terrestrial experiments. The following sections describe: analysis of the magnitude of thermogravitational, solutogravitational, thermocapillary and solutocapillary convection expected in rocket and ground testing; and a means for estimating mass transfer effects via heat and mass transfer analogies.

● Thermogravitational Dimensional Analysis

A schematic of the mixing experiment liquids is shown in Fig. 4. Dimensional analysis of this configuration requires that values of the Rayleigh and Marangoni numbers be calculated for both terrestrial and rocket conditions and then compared to the critical Rayleigh and Marangoni numbers. The aspect ratio (length-to-diameter) and Prandtl number of the processes are also important parameters. Ignoring the Marangoni effect for the present, the dimensional analysis for thermal buoyancy convection is presented in this section.

For heating from below or above (vertical processing) the Rayleigh number is defined as:

20

$$g = 1.0 \times 10^{-4} \, g_E$$

Rigid or
Free Boundaries
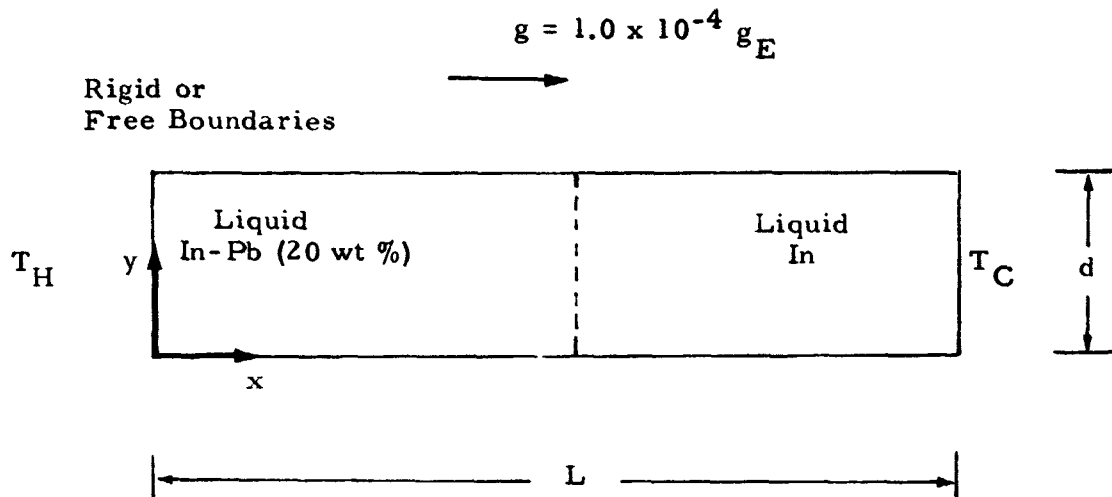
Thermal Conditions: Radial Temperature Gradient = 0.98 $^{\circ}$C/cm

Axial Temperature Gradient = 0.011 $^{\circ}$C/cm

Dimensions: L = 2.35 cm

d = 0.61 cm

Fig. 4 - Physical Model and Coordinate System
for InPb Experiment

21

$$Ra_L = \beta g \frac{(T_{Hot} - T_{Cold})}{\nu \alpha} L^3$$

where

β = thermal expansion coefficient

g = gravity level

ν = kinematic viscosity

α = thermal diffusivity

The mean gravity expected during the rocket coast phase is approximately 10^{-4} $g_E (g_E = 980$ cm/sec^2). Thus during vertical processing, $Ra_L \rfloor_{Earth} = 2.7$ and $Ra_L \rfloor_{Rocket} = 2.7 \cdot 10^{-4}$. The critical Rayleigh number, Ra_L^C, depends on the heating direction, aspect ratio (γ), and Prandtl number (Pr). For the mixing experiment, Pr = $8 \cdot 10^{-3}$ and $\gamma = L/D = 3.8$. Thus $Ra_L^C = 1.6 \cdot 10^4$ for heating from below (Ref. 9) and convection is not even likely in ground processing. $Ra_L^C = \infty$ for heating from above which means that convection is theoretically always absent. Actually, however, finite lateral temperature gradients exist (side heating or cooling); and Ra^C for side heating is zero (some flow always exists). In side heating, however, the heat and mass transport may not be increased until a second critical Rayleigh number, Ra_w^C, is reached.

For side heating (horizontal processing) the Rayleigh number is defined as,

$$Ra_w = \beta g (T_{Hot} - T_{Cold}) D^3 / \nu \alpha$$

and the critical Rayleigh number for convective heat and mass transport is defined as (Ref. 10).

$$Ra_w^C = 592 \gamma \sqrt{\gamma - 1} = 3.8 \cdot 10^3$$

For ground processing, $Ra_w = 1.1 \cdot 10^2$; while for the rocket, $Ra_w = 1 \ 1 \cdot 10^{-2}$.

Thus, utilizing a rocket mean gravity level of 10^{-4} g_E, the Rayleigh numbers are:

	Ground	Rocket
Ra_L/Ra_L^c	$2 \cdot 10^{-4}$	$2 \cdot 10^{-8}$
Ra_w/Ra_w^c	$3 \cdot 10^{-2}$	$3 \cdot 10^{-6}$

Therefore, thermal buoyancy convection is unlikely during ground or microgravity processing.

● Solutogravitational Dimensional Analysis

For freezing from below or above (vertical processing) the solutal Rayleigh number is defined as:

$$Ra'_L = \frac{\beta_c g \, \Delta C \, L^3}{\nu \mathfrak{D}}$$

where

$$\beta_c = \frac{1}{\rho}\left(\frac{\partial \rho}{\partial C}\right)_T$$

C = concentration of solute*

$\mathfrak{D}$ = molecular diffusivity of solute

Utilizing 10^{-4} g_E for rocket processing, solutal Rayleigh numbers for vertical processing are:*

Earth: $Ra'_L = 3.1 \cdot 10^9$

Rocket: $Ra'_L = 3.1 \cdot 10^5$

The critical solutal Rayleigh number, $Ra_L^{c'}$, depends on the freezing direction, aspect ratio, γ, and Schmidt number, Sc. For the mixing experiment,

---

*ΔC = 0.2 wt % Pb, L = 1.18 cm

23

$Sc = 170$ and $\gamma = L/D = 3.8$. Thus $Ra_L^{'c} = 5 \cdot 10^4$ for freezing from above (In-Pb segment in upper half of cylinder) (Ref. 9) and solutal convection is probable in both ground and rocket processing. $Ra_L^c = \infty$ for freezing from below (In-Pb segment in lower half of cylinder). This means that solutal convection is not possible in the latter configuration.

For side heating (horizontal processing) the solutal Rayleigh number is defined as:

$$Ra_w' = \beta_c g (\Delta C) D^3 / \nu \mathfrak{D}$$

and the critical Rayleigh number for convective heat and mass transport is defined as (Ref. 10).

$$Ra_w^{c'} = 592 \, \gamma \sqrt{\gamma - 1} = 3.8 \cdot 10^3$$

For ground processing, let $Ra_w' = 4 \cdot 10^8$; while for the rocket, let $Ra_w' = 4 \cdot 10^4$. Thus, utilizing a rocket mean gravity level of $10^{-4} \, g_E$, the solutal Rayleigh numbers are:

	Ground	Rocket
$Ra_L' / Ra_L^{c'}$	$6.2 \cdot 10^4$	6.2
$Ra_w' / Ra_w^{c'}$	$10.5 \cdot 10^4$	10.5

Thus, convection is likely during freezing from above processing on the ground and on the rocket; while horizontal processing will also yield convective influences during ground and rocket processing also.

● Thermocapillary Dimensional Analysis

Surface tension gradients may be an important source of convection in melts whenever a liquid-fluid interface is present (Ref. 11).

As with thermogravitational convection, thermocapillary flow will be laminar with small surface tension driving forces, oscillatory at moderate driving forces and turbulent at large driving forces. The ratio of capillary driving force to resisting viscous force is expressed by the Marangoni number defined as,

$$Ma_L = - \frac{\frac{d\sigma}{dT} \Delta T \ L}{\rho \nu \alpha}$$

for temperature gradients parallel to the liquid-fluid interface and as

$$Ma_w = - \frac{\frac{d\sigma}{dT} \Delta T \ w}{\rho \nu \alpha}$$

for temperature gradients perpendicular to the liquid-fluid interface. The symbol σ represents the surface tension and $d\sigma/dT = -0.08 \ dyn/cm^\circ C$ for InPb (Ref. 12).

A critical Marangoni number has been established for Ma_w (Ref. 13), but not for Ma_L. Values of Ma_L, Ma_w and Ma_w^c are shown below.

$$Ma_L = 2.85$$

$$Ma_w = 1.95, \ Ma_w^c = 70$$

Even though no firm critical Ma_L is known, values of $Ma_L \geq 7$ exhibited oscillatory laminar flow and $Ma_L \geq 140$ indicated turbulent flow for molten silicon (Ref. 11). It is therefore evident that significant thermocapillary flow should not occur in the mixing experiment.

It should be mentioned at this point, however, that little or no data exist on values of $d\sigma/dT$ in the presence of dopants or of oxide films (see Appendix

25

C, Ref. 14). Neither the preceding Marangoni numbers nor the analysis by Chang and Wilcox (Ref. 11) account for these phenomena. Thick oxide films may completely suppress thermocapillary convection.

● Solutocapillary Dimensional Analysis

No explicit data exists on values of $d\sigma/dC$ for the In-Pb system. Esimating $d\sigma/dC$ from Hoar and Melford (Ref. 12) the solutal Marangoni numbers, Ma'_L and Ma'_w, are as follows:

● For concentration gradients parallel to the liquid-fluid interface,

$$Ma'_L = \frac{\frac{d\sigma}{dC} \Delta CL}{\rho \nu a} = 1.7 \cdot 10^8$$

● For concentration gradients perpendicular to the liquid-fluid interface.

$$Ma'_w = \frac{\frac{d\sigma}{dC} \Delta CD}{\rho \nu a} = 2.2 \cdot 10^7$$

Thus solutocapillary convection may be significant on the rocket.

● Heat and Mass Transfer Rates

Convection affects solidification from the melt primarily through its influence on (Ref. 15): (1) the amount of dopant or impurity delivered to the vicinity of the solid-liquid interface; i.e., the rate of mass transfer; and (2) the temperature fluctuations cuused near the growth interface (heat transfer). A convenient measure of the convective augmentation to heat transfer is the Nusselt number, Nu. It represents the ratio of total heat transfer to conduction heat transfer and is defined as

$$Nu = hL/k$$

26

where h is an overall coefficient of heat transfer. It is related to thermal and concentration driving forces as follows

$$Nu = C_1 \, Ra^{C_2} + C_3 \, Ma^{C_4} + C_5 \, Ra^{C_6} + C_7 \, Ma^{C_8}$$

where the C_i's are constants.

The constants, C_i, sometimes incorporate the effects of geometry via the aspect ratio, γ, and the effects of relative diffusivity via the Pr and Sc numbers. The Prandtl number is the ratio of momentum diffisivity, ν, to thermal diffusivity, α. For solutal convection, the Schmidt number, Sc, rather than Pr is important. The Schmidt number is the ratio of momentum diffusivity to molecular diffusion (Sc $= \nu/\mathfrak{D}$).

Transport by convection tends to dominate as Pr or Sc becomes large. These two parameters are also important when estimating mass transfer rates from measured heat transfer rates and vice versa (Ref. 17). The degree of convective augmentation to mass transport is reflected by the Sherwood number, Sh, which is analogous to Nu. For small flow rates, the Sherwood, Nusselt, Schmidt, and Prandtl numbers are related as follows

$$\frac{Sh}{Nu} = \left(\frac{Sc}{Pr} \right)^n$$

where $n \approx 1/2$ for laminar flow and $n \approx 1/3$ for turbulent flow. The analogy between heat and mass transfer can be utilized to estimate mass transfer rates from computed heat transfer rates or vice-versa. Furthermore, the Nusselt and Sherwood numbers can be related as follows for vertical processing (Ref. 16):

27

$$Nu_L = 1 + .14 \left[Ra_L + Ra'_L Le^{-16/11} \right]^{3/8}$$

$$Sh_L = 1 + (Nu_L - 1) Le^{6/11}$$

where Le = Lewis number = Sc/Pr. For freezing from above in the mixing experiment

$$Le = 2.5 \cdot 10^4$$

$$Nu_L = 1.04$$

$$Sh_L = 17.6$$

Thus convective mixing, generated primarily by concentration gradients, should lead to significant transport of solute relative to the rate of pure diffusion, even though convective heat transfer augmentation is minor ($Nu \approx 1$).

● Conclusions

Sensitivity calculations indicate that thermogravitational convection will not be important in ground or rocket processing. Solutogravitational flow should be significant even for rocket processing. Thermocapillary flow should be negligible in both ground and rocket testing. Solutocapillary convection may also be significant, if the Pb-In concentration gradient were to exist at a liquid-vapor interface.

1.8 CONVECTION MODELING

Results in this subsection are directed toward the theoretical prediction of the mixing experiment results. The ability to analytically model the experiment is essential for analysis of the sounding rocket flight data. The following is a description of the configuration analyzed and of some flight results that have been obtained.

The basic portion of the experiment consists of three orthogonal cylinders each of which contain indium and an indium-lead alloy. The metals are melted and held in the molten state for about four minutes. A complete description of the cylinder design, heat-up etc., is given in Section 1.1. For the purpose of analysis the configuration in Fig. 5 is used.

In Fig. 5:

   w = mass concentration of indium
   T = temperature
   ϵ = jitter component of gravitational field
   g_e = earth gravity
   λ = wavelength of "sawtooth" g-jitter

The definitions of other variables and parameters in Fig. 5 are obvious.

The gravitational field and the time variations shown are the result of studying the accelerometer data from the 4 October 1974 sounding rocket flight. The "sawtoo..." jitter with an amplitude and frequency roughly equal to the average of the flight data was chosen to represent the g-field variations.

The Lockheed Convection Analysis program was used to predict the mixing for the configuration in Fig. 5. The cylinder could not be analyzed for the situation given in Fig. 5 because the flow field is three-dimensional. Thus a rectangular box was analyzed to obtain some qualitative results. The phenomena assumed to be driving the mixing are diffusion and buoyancy.
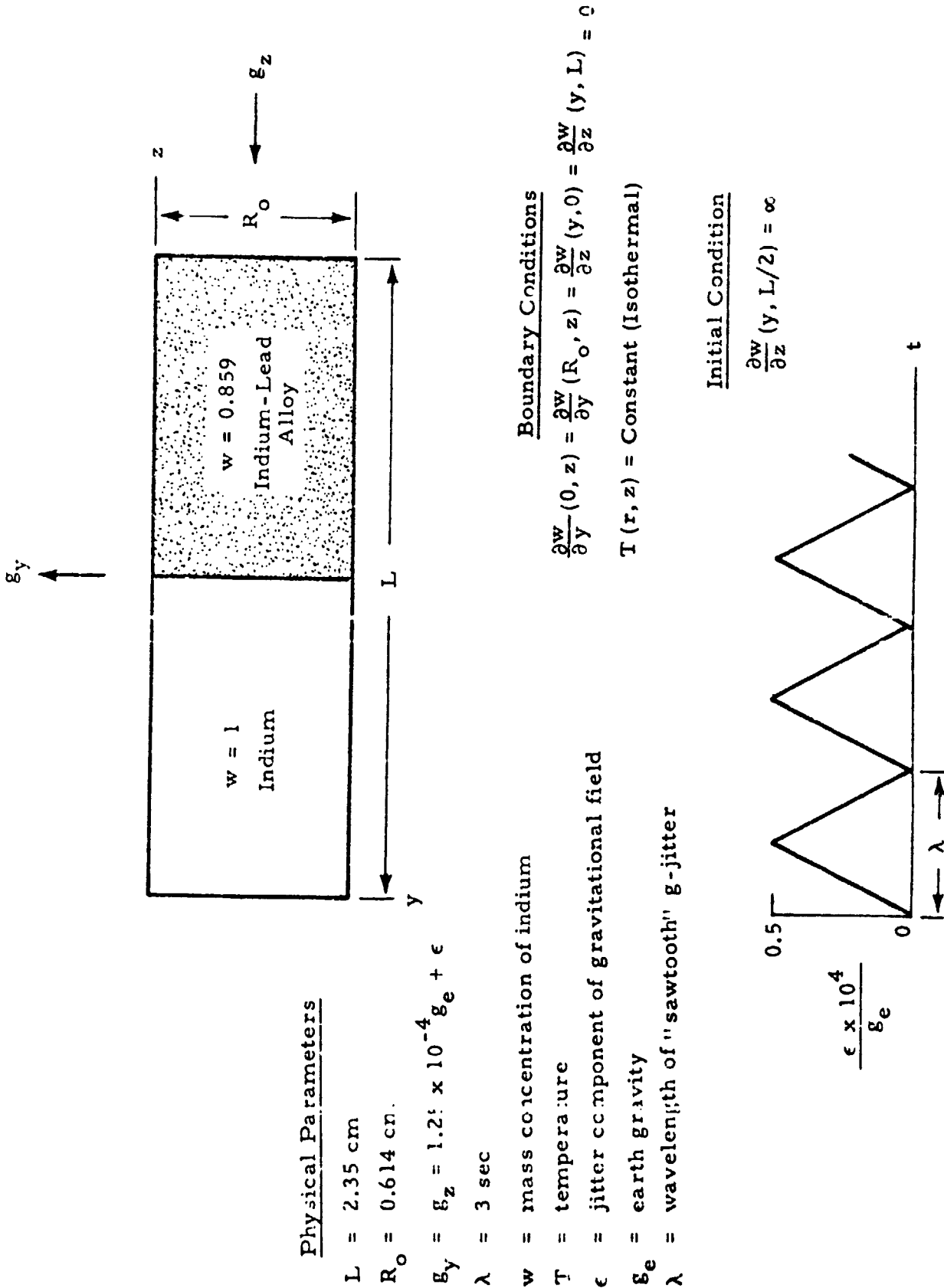
29

g_z

z

R_o

g_y

w = 0.859
Indium-Lead
Alloy

w = 1
Indium

L

y

Physical Parameters

$L = 2.35$ cm

$R_o = 0.614$ cn.

$g_y = g_z = 1.2^{5} \times 10^{-4} g_e + \epsilon$

$\lambda = 3$ sec

w = mass concentration of indium

T = temperature

ϵ = jitter component of gravitational field

g_e = earth gravity

λ = wavelength of "sawtooth" g-jitter

Boundary Conditions

$\frac{\partial w}{\partial y}(0, z) = \frac{\partial w}{\partial y}(R_o, z) = \frac{\partial w}{\partial z}(y, 0) = \frac{\partial w}{\partial z}(y, L) = 0$

$T(r, z) = $ Constant (Isothermal)

Initial Condition

$\frac{\partial w}{\partial z}(y, L/2) = \infty$

$\frac{\epsilon \times 10^4}{g_e}$

0.5

0

λ

t

Fig. 5 - Configuration for Experiment Analysis

30

LOCKHEED · HUNTSVILLE RESEARCH & ENGINEERING CENTER

For the gravity levels used, the analysis indicates that mixing may occur as far as 0.5 cm from the initial indium/indium-lead interface as a result of buoyancy. The mixing is expected to be approximately as shown in Fig. 6.
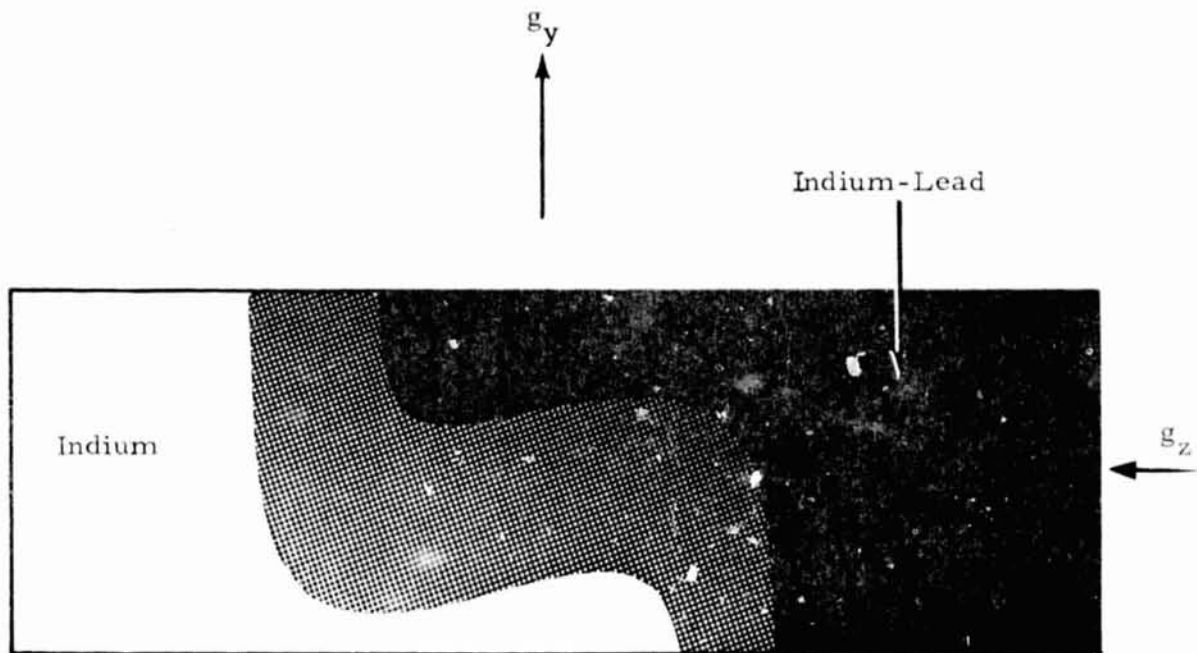
31

Fig.6 - Mixing of Molten Indium and Indium-Lead After 3 Minutes in a 10^{-4}g Gravitational Field

Section 2
POSTFLIGHT ANALYSES

2.1 INTRODUCTION

This section contains results of postflight convection sensitivity and modeling analyses. These studies were conducted to assist the Principal Investigator to interpret rocket flight results. The rocket flight results, both estimated g-levels and mixing, are shown in Figs. 7, 8 and 9. Results show that no flow was experienced in the sample mounted parallel to the rockets longitudinal axis. One of the samples mounted in a plane perpendicular to the rocket's longitudinal axis experienced a very small motion of the interface. The other sample (in the same plane) experienced flow down one side of the sample container. The maximum gravity levels were estimated to be 2.10^{-5} g (Ref. 19). Thus significant mixing and complete reorientation of the lead phase occurred in Flight Sample No. 6, but no significant mixing occured in the other two flight samples.

2.2 CONVECTION SENSITIVITY

The convection sensitivity analysis of Section 1.7 has been updated to account for actual rocket acceleration levels and for an important, recent contribution (Ref. 18) to the state-of-the-art in the theory of convection onset. Nield (Ref. 18) has evaluated the effects of nonlinear, vertical density profiles on the onset of convection (critical Rayleigh number, Ra_c). In particular, he predicts that a step function change in density at the mid-height of the container will reduce Ra_c to 60% of its value for a linear density profile. Applying this result (in conjunction with the sensitivity criteria of Section 1.7.3) to the rocket results (as given by Table 3), indicates that rocket sample No. 6 should have indeed showed the greatest tendency toward mixing. Furthermore, it is important to note that the effect of step-function density
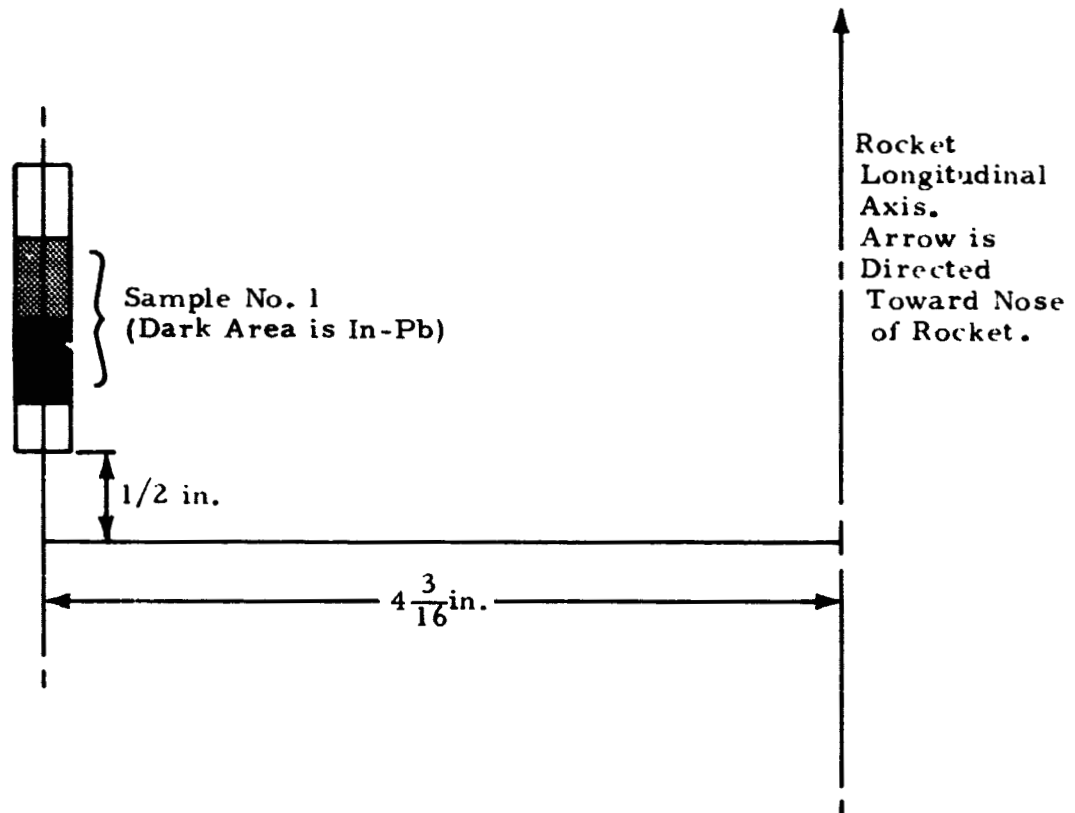
33

Rocket
Longitudinal
Axis.
Arrow is
Directed
Toward Nose
of Rocket.

Sample No. 1
(Dark Area is In-Pb)

1/2 in.

$4\frac{3}{16}$ in.

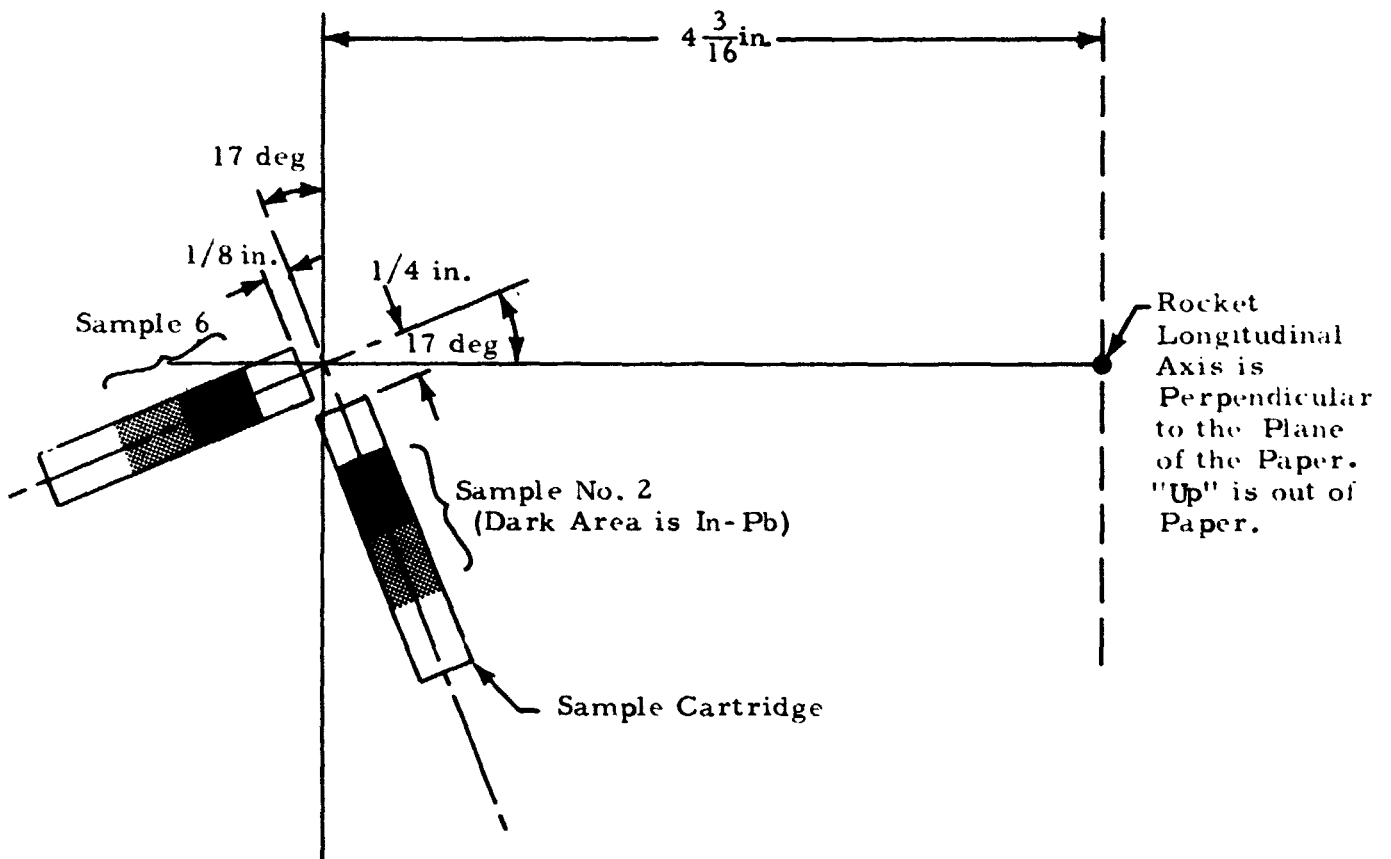Fig. 7 - Orientation of Sample No. 1

34

LOCKHEED · HUNTSVILLE RESEARCH & ENGINEERING CENTER

Fig. 8 - Orientations of Sample Nos. 2 and 6

LOCKHEED - HUNTSVILLE RESEARCH & ENGINEERING CENTER
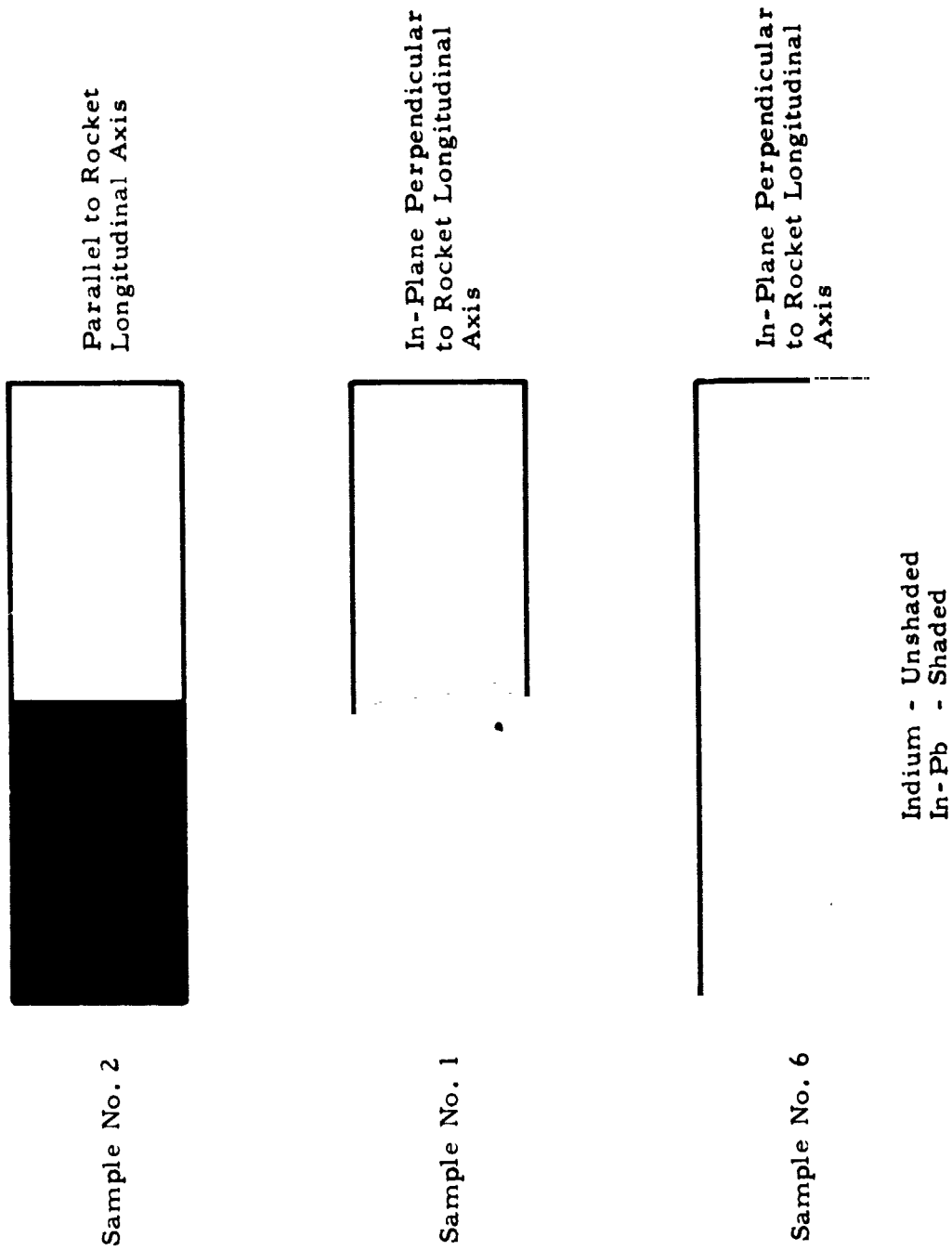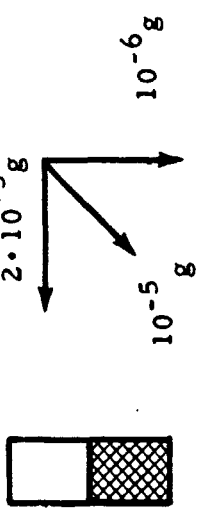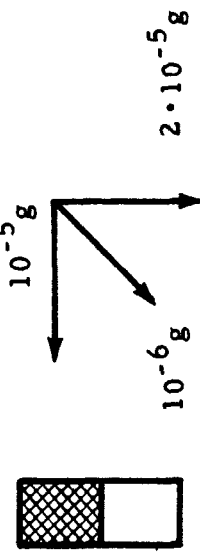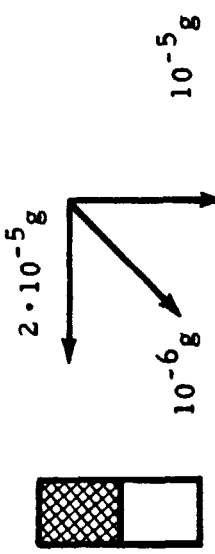
Fig. 9 - Appearance of Sample Interfaces (Ref. 19)

Parallel to Rocket Longitudinal Axis

Sample No. 2

In-Plane Perpendicular to Rocket Longitudinal Axis

Sample No. 1

In-Plane Perpendicular to Rocket Longitudinal Axis

Sample No. 6

Indium - Unshaded
In-Pb - Shaded

Table 3

ROCKET EXPERIMENT 74-18 CONVECTION SENSITIVITY*

Rocket Sample Number	Configuration** and Estimated Mean Gravity Values (g = 980 cm/sec^2)	Ra_L/Ra^c_L (Linear Profile)	Ra_L/Ra^c_L (Step Function Profile)	Ra_w/Ra^c_w (Linear Profile)
1	$2\cdot10^{-5}$ g, 10^{-6} g, 10^{-5} g	0.1 @ 10^{-6} g	0.2 @ 10^{-6} g	1.2 @ $2\cdot10^{-5}$ g 0.6 @ 10^{-5} g
6	10^{-5} g, $2\cdot10^{-5}$ g, 10^{-6} g	1.2 @ $2\cdot10^{-5}$ g	2.1 @ $2\cdot10^{-5}$ g	0.6 @ 10^{-5} g 0.1 @ 10^{-6} g
2	$2\cdot10^{-5}$ g, 10^{-5} g, 10^{-6} g	0.6 @ 10^{-5} g	1.1 @ 10^{-5} g	1.2 @ $2\cdot10^{-5}$ g 0.1 @ 10^{-6} g

*Ra_L is the solutal Rayleigh number for vertical processing, while Ra_w is the solutal Rayleigh number for horizontal processing.

**Cross hatched areas indicate In-Pb.

profiles on Ra_w^c is unknown. Therefore $Ra_w/Ra_w^c \gg 1$ (which indicates mixing) shown in Table 3 may not be valid. This further reinforces that mixing should have occurred in rocket sample No. 6 and not in the other rocket samples.

2.3 CONVECTION MODELING

The Lockheed Convection Computer program was used to model and analyze the rocket results. The initial and boundary conditions utilized for these models are identical to those of Fig. 5 except for gravity. The model results and g-levels used are shown in Figs. 10, 11 and 12. These figures show that no significant mixing occurred in any of the rocket samples. The melt velocities computed were less than 0.001 cm/sec for all the cases. Thus the extreme mixing demonstrated in Flight Sample No. 6 must have been due to surface tension forces or buoyancy forces larger than used in the computer analysis.

The computer analysis is limited in accuracy by its inability to account for three-dimensional flows (two-dimensional flow in rectangles modeled). It is believed that gravity levels shown for Sample No. 6 in Table 3, rather than those shown in Fig. 12 (for Sample No. 6), are more characteristic of actual flight conditions and would result in model results consistent with the flight results shown in Fig. 9.

Surface tension forces could also have given rise to mixing if the In/In-Pb interface ever existed along a liquid/vapor free surface. This could only occur if the melt pulled away from the cylinder wall at the mid-length of the container. This is an unlikely occurrence.

In conclusion, it is felt that mixing in Flight Sample No. 6 was caused by gravity levels and directions not currently accounted for (in conjunction with solutally induced density gradients). Therefore, further analysis of flight accelerations and additional computer model simulations (using other gravity conditions) are recommended.
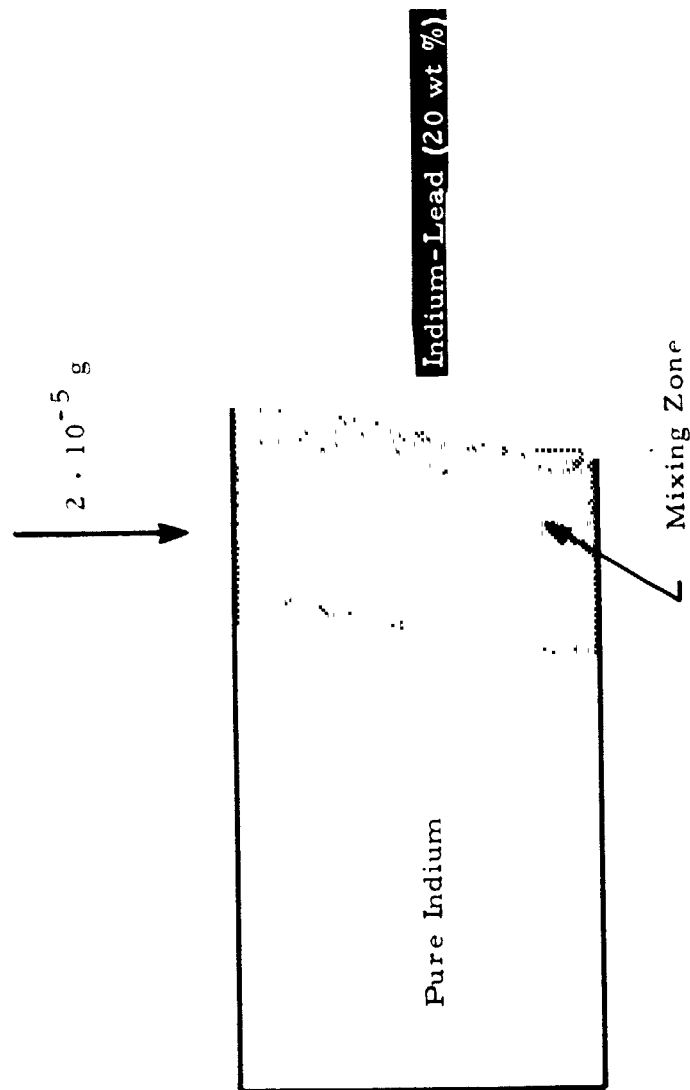
38

Fig. 10 - Computer Simulation of Mixing in Rocket Experiment 74-18 (Flight Sample No. 1, 180 sec after melting)
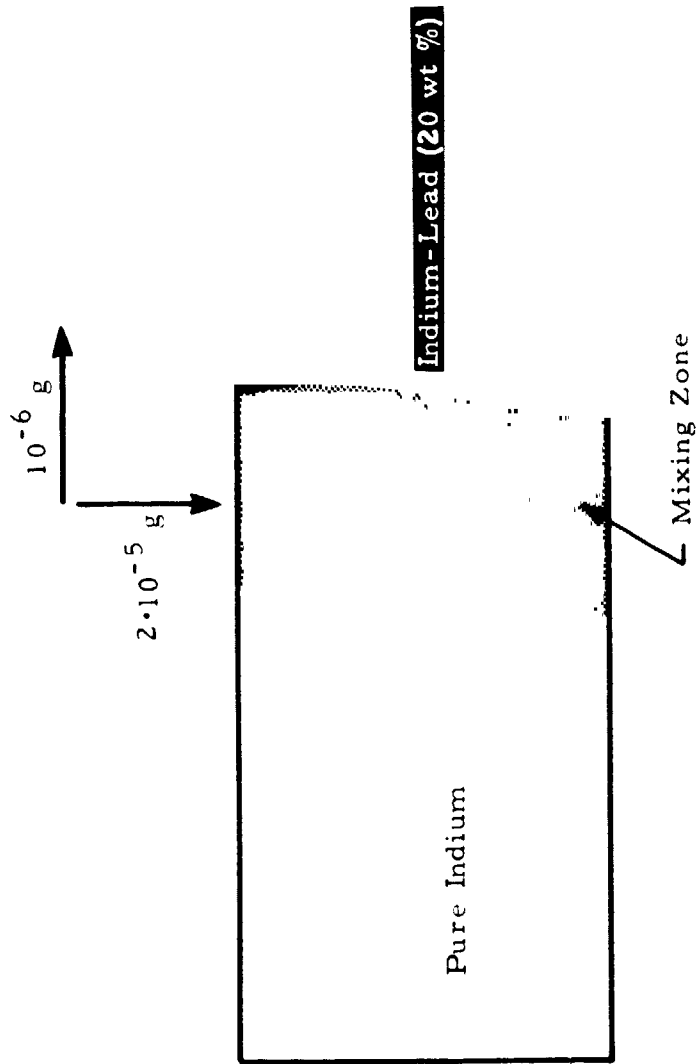
Fig. 11 - Computer Simulation of Mixing in Rocket Experiment 74-18 (Flight Sample No. 2, 170 sec after melting)
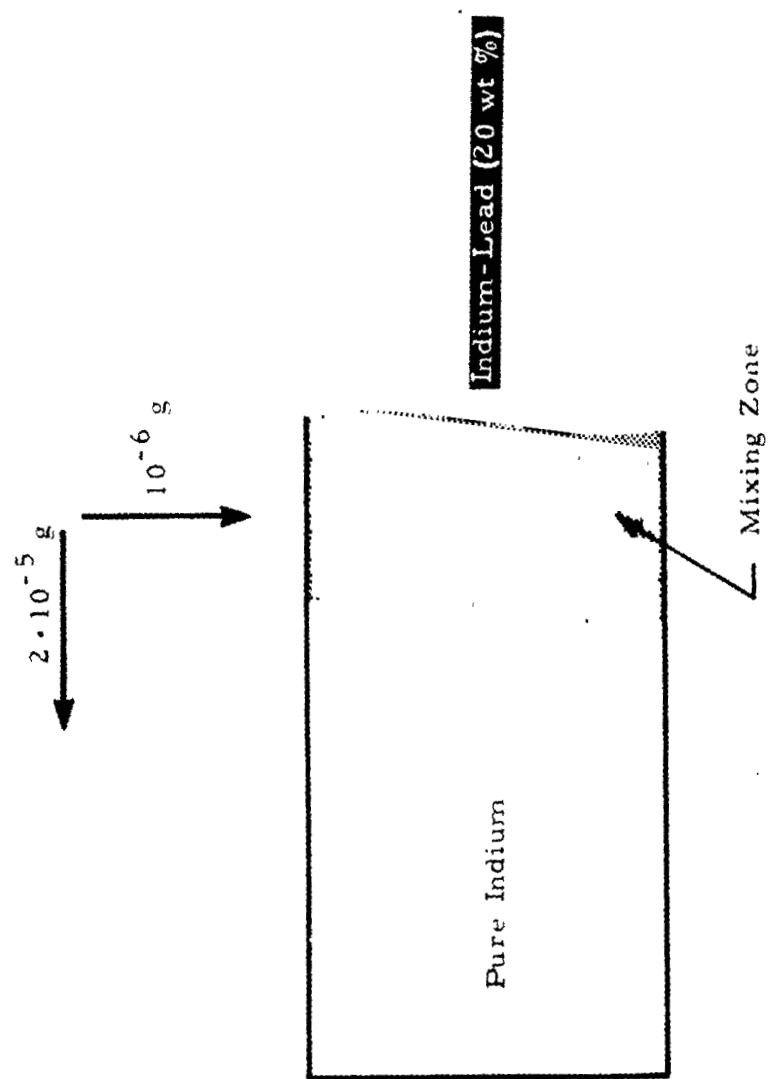
Indium-Lead (20 wt %)

$2 \cdot 10^{-5}$ g

10^{-6} g

Pure Indium

Mixing Zone

Fig. 12 - Computer Simulation of Mixing in Rocket Experiment 74-18 (Flight Sample No. 6, 175 sec after melting)

REFERENCES

1. Lovin, Juan K., "Lockheed-Huntsville Thermal Analyser," LMSC-HREC D225095, Lockheed Missiles & Space Company, Huntsville, Ala., July 1972.

2. Lyon, Richard N., Liquid-Metals Handbook, AEC and Bureau of Ships, Department of the Navy, Washington, D. C.

3. Beer, Sylvan Z., Liquid Metals Chemistry and Physics, Marcel-Dekker, New York, 1972.

4. Smithells, Metals Reference Book, Butterworths, London, 1962.

5. Weast, Robert C., Handbook of Chemistry and Physics, 51st Edition, The Chemical Rubber Company, Akron, Ohio, 1971.

6. Bird, R. B., W. F. Stewart and E. N. Lightfoot, Transport Phenomena, Wiley, New York, 1960, pp. 412-414.

7. Ede, A. J., "Advances in Free Convection," in Adv. Heat Trans., Vol. 4, 1967, pp. 1-64.

8. Ostrach, S., in "High Speed Aerodynamics and Jet Propulsion," F. K. Moore, ed., Vol. 4, Chapter F, Princeton University Press, Princeton, N. J., 1964.

9. Catton, I., "Effect of Wall Conduction on the Stability of a Fluid in a Rectangular Region Heated from Below," J. Heat Transfer, November 1972, p. 451.

10. Cormack, D. E., L. G. Leal and J. Imberger, "Natural Convection in a Shallow Cavity with Differentially Heated End Walls," J. Fluid Mech., Vol. 65, 1974, p. 227.

11. Chang, C. E., and W. R. Wilcox, "Inhomogeneities Due to Thermocapillary Flow in Floating Zone Melting," J. Crystal Growth, Vol. 28, 1975, pp. 8-12.

12. Hoar, T. P. and D. A. Melford, "The Surface Tension of Binary Liquid Mixtures: Pb-In Alloys," Trans. Faraday Soc., Vol. 53, 1957, p. 315.

13. Pearson, J. R. A., "On Convection Cells Introduced by Surface Tension," J. Fluid Mech., Vol. 4, 1958, p. 489.
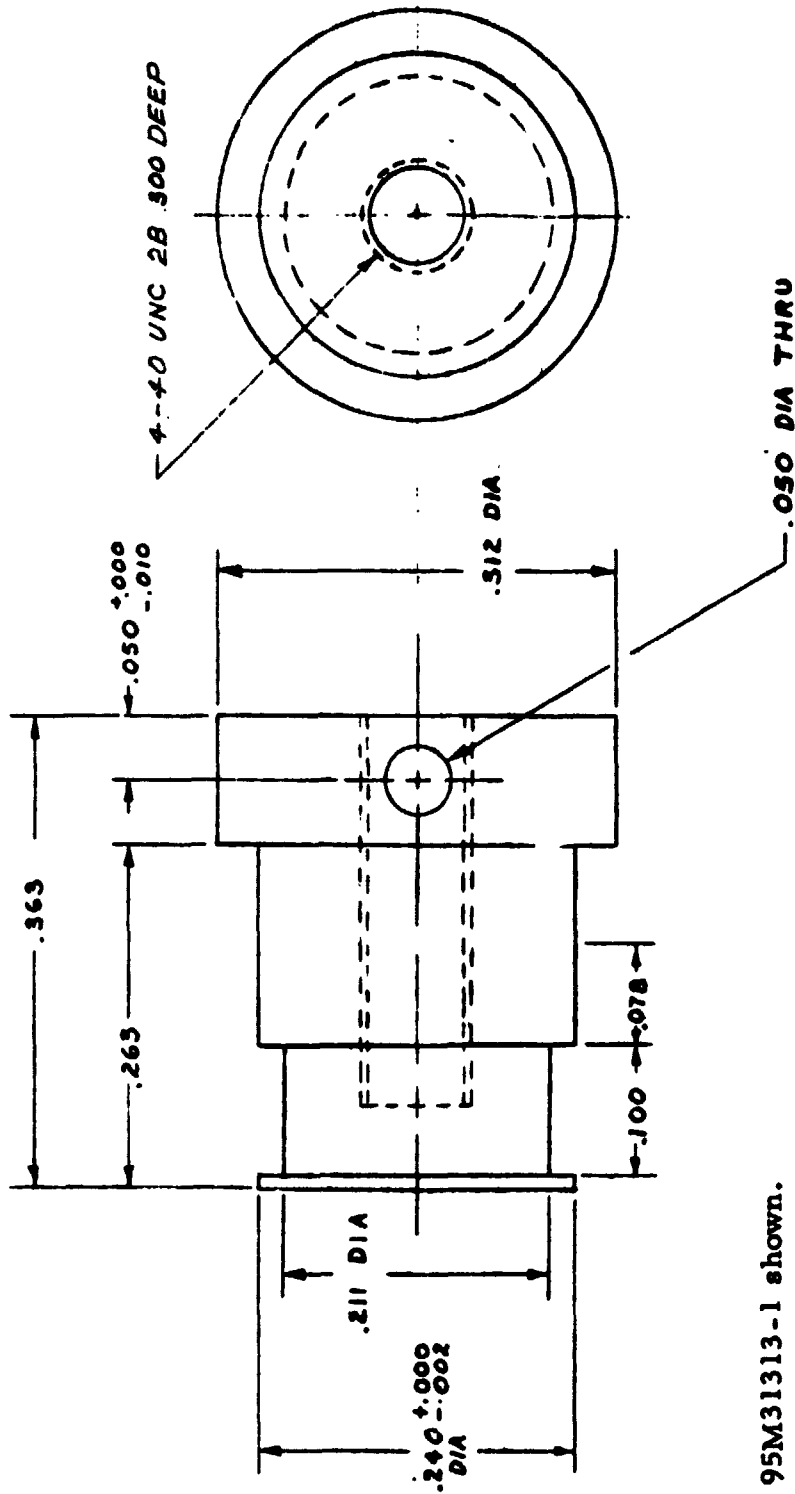
14. Bourgeois, S. V., and L. W. Spradley, "Skylab M518 Multipurpose Furnace Convection Analysis," LMSC-HREC TR D496534, Lockheed Missiles & Space Company, Huntsville, Ala., September 1975.

15. Carruthers, J. R., "Thermal Convection Instabilities Relevant to Crystal Growth from Liquids," in Preparation and Properties of Solid State Materials, Vol. 2, ed. W. R. Wilcox, Marcel Dekker, New York, 1975.

16. Lindberg. W. R. , and R. D. Haberstroh, AICHE J., Vol. 18, 1972, pp. 243-245.

17. Bird, R., W. Stewart and E. Lightfoot, Transport Pheomena, John Wiley, New York, 1960, p. 646.

18. Nield, D. A., "The Onset of Transient Convective Instability," J. Fluid Mech., Vol. 71, 1975, pp. 441-454.

19. Schafer, C. S., Private Communication, April 1976.

43

Appendix

ENGINEERING DRAWINGS

NOTES:

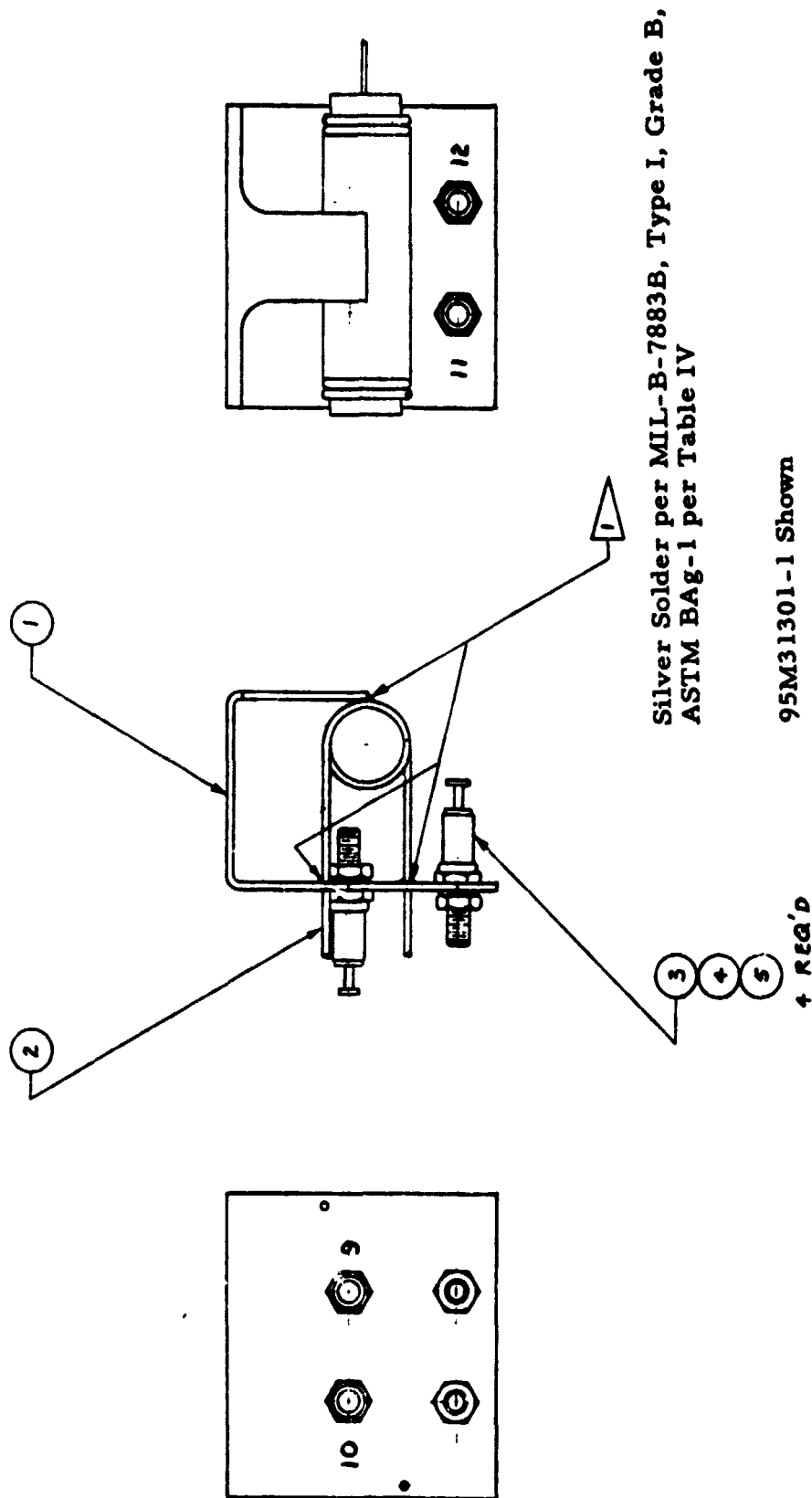1. Remove all burrs and break sharp edges.
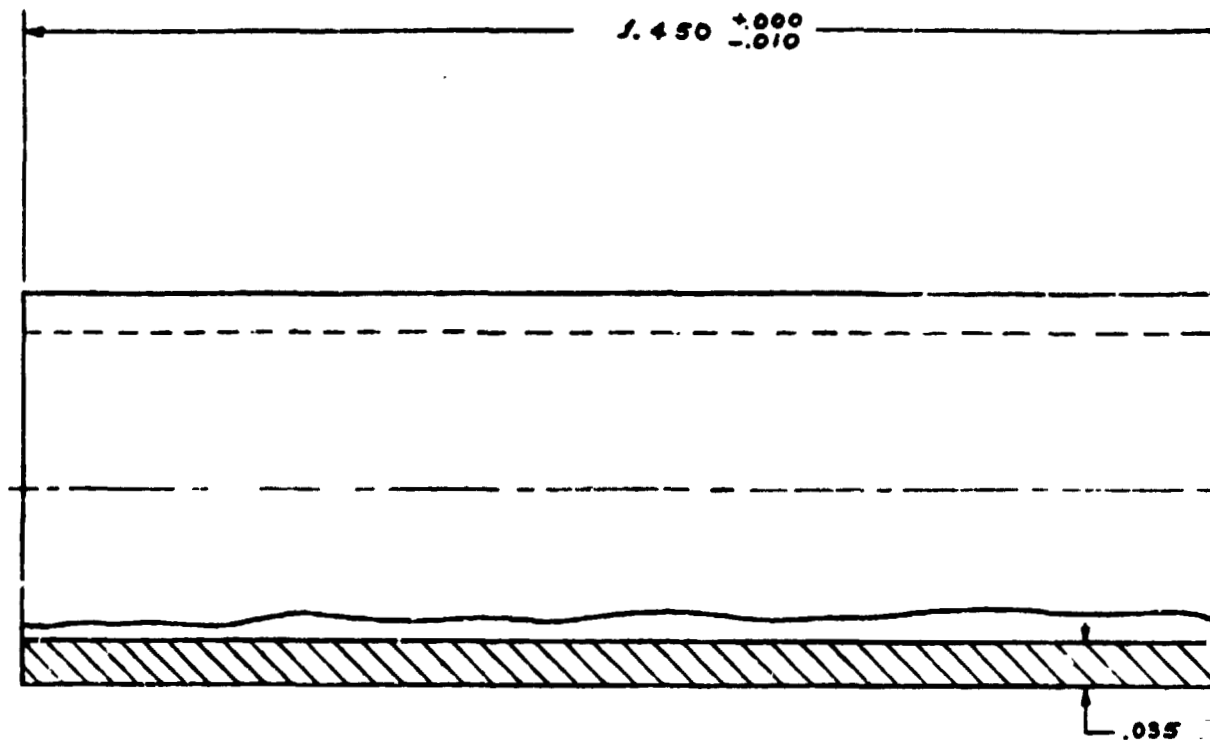2. Material: Aℓ alloy 6061-T6-PER.WW-T-700/6; 0.035 wall thickness.

4--40 UNC 2B .300 DEEP

.050 DIA THRU

.512 DIA

.050 +.000 / -.010

.363

.265

.100 → ←.078

.211 DIA

.240 +.000 / -.002 DIA

95M31313-1 shown.

Tube Heater Coil (from MSFC Dwg. 95M31313)

A-1

Silver Solder per MIL-B-7883B, Type I, Grade B,
ASTM BAg-1 per Table IV

95M31301-1 Shown

Single Heater Assembly (from MSFC Dwg. 95M31309)

A-2

95M31313-1 Shown

$1.450 \begin{smallmatrix} +.000 \\ -.010 \end{smallmatrix}$

.035

NOTES:

1. Remove all burrs and break sharp edges.

2. Material, Al Aly. 6061-T6-DER.WW-T-700/6.
   — 0.035 wall thickness

.312
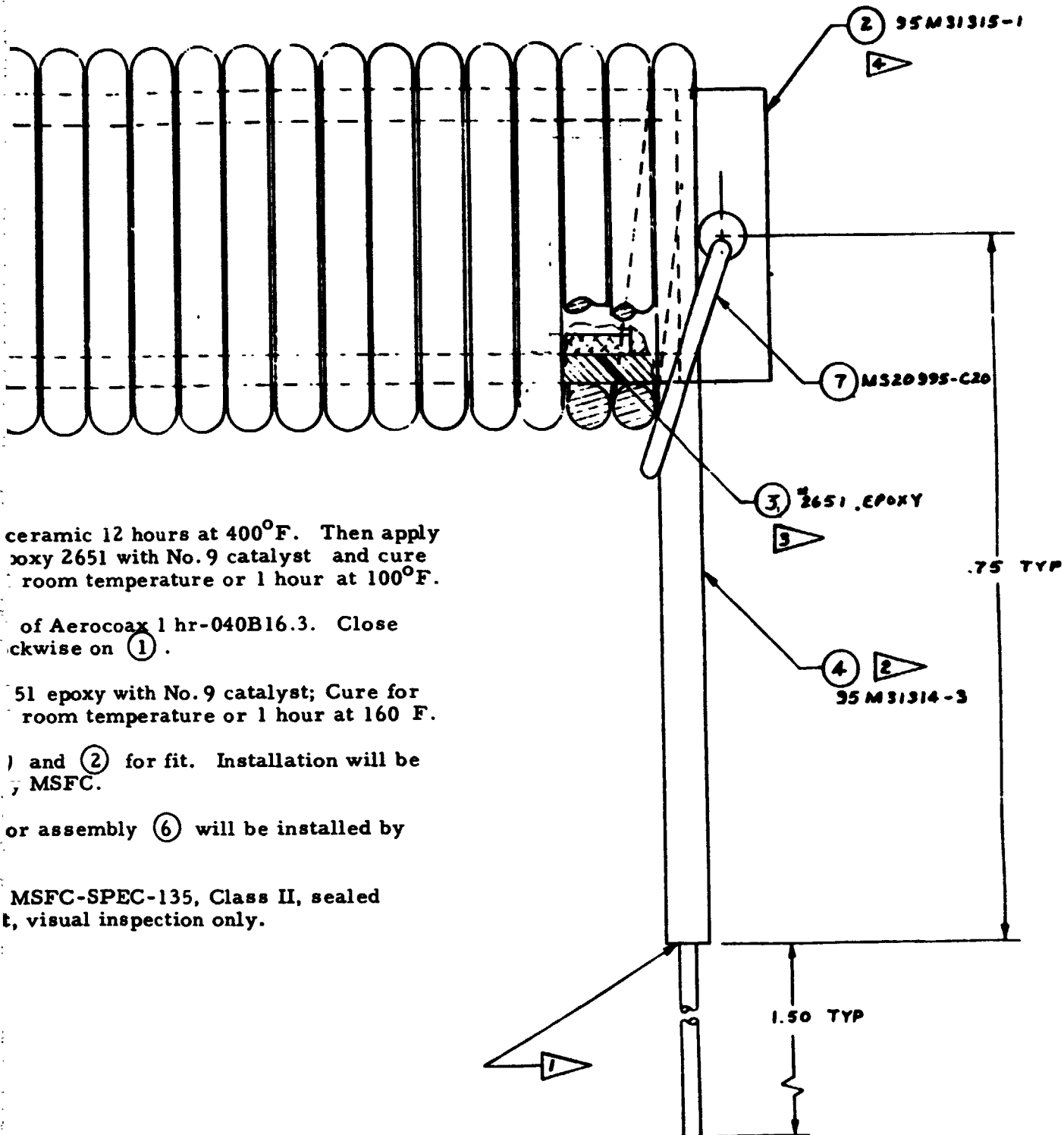DIA

.035 REF

.95M31313

Tube Heater Coil

A-3

① 95M31313-1

⑥ 20536-1

95M31312-1 ⑤

③ REF

NOTES:

1 ▷ Bake out ceramic 12 hours
Stycast Epoxy 2651 with No
8 hours at room temperatu:

2 ▷ 29.5 turns of Aerocoax 1 hr
wound clockwise on ① .

3 ▷ Stycast 2651 epoxy with No
8 hours at room temperatu:

4 ▷ Check ① and ② for fit.
made at by MSFC.

5 ▷ Thermistor assembly ⑥
MSFC.

6 ▷ Weld per MSFC-SPEC-135
weld joint, visual inspecti

FOLDOUT FRAME 1
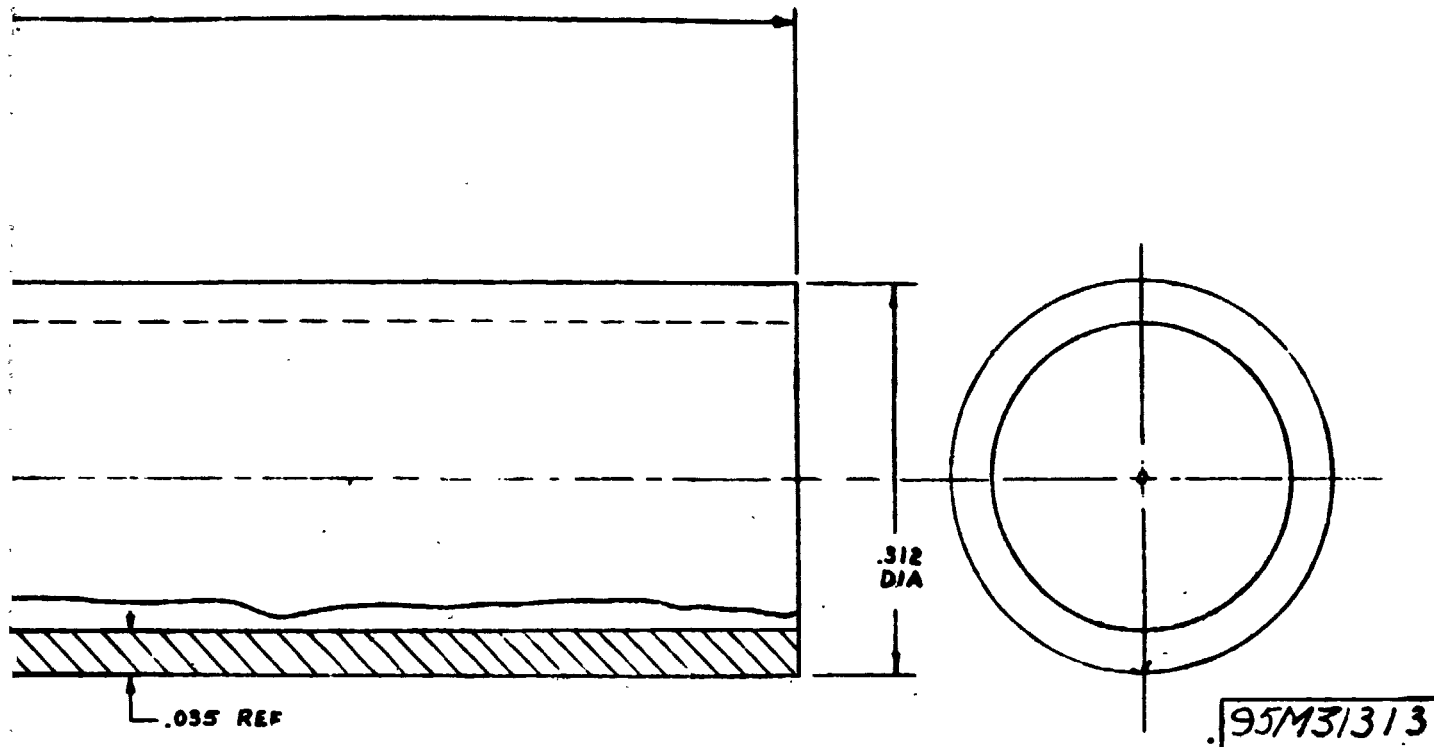
ceramic 12 hours at 400°F. Then apply
poxy 2651 with No. 9 catalyst and cure
room temperature or 1 hour at 100°F.

of Aerocoax 1 hr-040B16.3. Close
ckwise on ①.

51 epoxy with No. 9 catalyst; Cure for
room temperature or 1 hour at 160 F.

) and ② for fit. Installation will be
, MSFC.

or assembly ⑥ will be installed by

MSFC-SPEC-135, Class II, sealed
t, visual inspection only.

Heater Coil Assembly